

## INFORMATION TO USERS

This manuscript has been reproduced from the microfilm master. UMI films the text directly from the original or copy submitted. Thus, some thesis and dissertation copies are in typewriter face, while others may be from any type of computer printer.

**The quality of this reproduction is dependent upon the quality of the copy submitted.** Broken or indistinct print, colored or poor quality illustrations and photographs, print bleedthrough, substandard margins, and improper alignment can adversely affect reproduction.

In the unlikely event that the author did not send UMI a complete manuscript and there are missing pages, these will be noted. Also, if unauthorized copyright material had to be removed, a note will indicate the deletion.

Oversize materials (e.g., maps, drawings, charts) are reproduced by sectioning the original, beginning at the upper left-hand corner and continuing from left to right in equal sections with small overlaps. Each original is also photographed in one exposure and is included in reduced form at the back of the book.

Photographs included in the original manuscript have been reproduced xerographically in this copy. Higher quality 6" x 9" black and white photographic prints are available for any photographs or illustrations appearing in this copy for an additional charge. Contact UMI directly to order.

# UMI

A Bell & Howell Information Company  
300 North Zeeb Road, Ann Arbor MI 48106-1346 USA  
313/761-4700 800/521-0600





Université d'Ottawa • University of Ottawa



THE EFFECTS OF DI- AND TRIACYLGLYCEROLS  
ON THE CHARGE, STABILITY AND CONFORMATION OF HDL  
AND ON HEPATIC LIPASE ACTIVITY

CYNTHIA ROSE COFFILL

Thesis submitted to the Department of Biochemistry in partial fulfillment  
of the requirement for the degree of Masters in Science

University of Ottawa  
Ottawa, Ontario, Canada  
August, 1998

© Cynthia Rose Coffill, Ottawa, Canada, 1998



National Library  
of Canada

Acquisitions and  
Bibliographic Services

395 Wellington Street  
Ottawa ON K1A 0N4  
Canada

Bibliothèque nationale  
du Canada

Acquisitions et  
services bibliographiques

395, rue Wellington  
Ottawa ON K1A 0N4  
Canada

*Your file Votre référence*

*Our file Notre référence*

The author has granted a non-exclusive licence allowing the National Library of Canada to reproduce, loan, distribute or sell copies of this thesis in microform, paper or electronic formats.

The author retains ownership of the copyright in this thesis. Neither the thesis nor substantial extracts from it may be printed or otherwise reproduced without the author's permission.

L'auteur a accordé une licence non exclusive permettant à la Bibliothèque nationale du Canada de reproduire, prêter, distribuer ou vendre des copies de cette thèse sous la forme de microfiche/film, de reproduction sur papier ou sur format électronique.

L'auteur conserve la propriété du droit d'auteur qui protège cette thèse. Ni la thèse ni des extraits substantiels de celle-ci ne doivent être imprimés ou autrement reproduits sans son autorisation.

0-612-36675-8

**Canada**

## ABSTRACT

Alterations in HDL composition that occur in the hypertriglyceridemic state may modulate a number of events involved in cholesterol homeostasis. To elucidate the details of how HDL neutral acylated glycerol (NAG) composition can affect the molecular structure of HDL particles, the charge, conformation and stability of apoA-I have been investigated in homogeneous recombinant HDL particles (Lp2A-I) containing phosphatidylcholine (POPC), triolein (TG) and/or diolein (DG). A spherical reconstituted particle containing 2 molecules of apoA-I and 120 molecules of phospholipid (PL) has a surface potential of -9.1 mV,  $\alpha$ -helix content of 62% and a thermodynamic stability ( $\Delta G_D^\circ$ ) of 1.4 kcal/mol apoA-I. Inclusion of 20-40 molecules of TG increases slightly the  $\alpha$ -helical content and  $\Delta G_D^\circ$  of apoA-I while lowering the surface potential. Epitopes located within the N-terminus of apoA-I are less exposed to the monoclonal antibodies (mAb) 4H1 and A17 in the presence of 40 molecules of TG. Inclusion of 20-40 molecules of DG causes increases in the  $\alpha$ -helix to 69% and the  $\Delta G_D^\circ$  to 2.1 kcal/mol apoA-I while lowering the surface potential to -11 mV. When both TG and DG are present in Lp2A-I, the particle charge and stability are proportional to the amount of DG present. The epitope recognized by mAb A51 is more exposed whereas the binding of mAb A11 to apoA-I is reduced in the presence of both these lipids. Lp2A-I enriched in DG exhibit charge and structural properties similar to that of  $\alpha$ -migrating HDL (-10.5 mV to -12.5 mV). Increases in DG content also induce the greatest change in conformation of apoA-I. Two epitopes situated at residues 126-132 and 149-186 exhibit a reduced exposure to mAb A11 and A44, in the presence of elevated DG levels.

The effect of HDL composition and structure on the hydrolysis of HDL phospholipids, DG and TG by hepatic lipase (HL) has also been investigated in native and Lp2A-I. Fasting, normolipidemic HDL exhibit total lipid hydrolytic rates of between 10 and 36 nM FA/h/ $\mu$ M PL. Of the total fatty acids liberated from HDL<sub>3</sub>, only 1% are from triolein (TG), while 49% are from diolein (DG) and 50% are from PL. A spherical reconstituted particle with 120 molecules of PL, 20 TG and 2 apoA-I exhibits a total lipid hydrolytic rate of 7 nM FA/h/ $\mu$ M PL and 74% of the fatty acids liberated are from PL. Inclusion of 40 molecules of TG into the Lp2A-I particle doubles the rate of fatty acid hydrolysis from TG. Further addition of 10 molecules of DG to the Lp2A-I complex has no effect on the overall rates of hydrolysis, but changes the substrate specificity, wherein 61% of the fatty acids are from DG and both TG and PL hydrolytic rates are significantly reduced. Increasing the amount of DG in the Lp2A-I particle further stimulates total lipid hydrolysis by raising DG hydrolytic rates at the expense of PL and TG hydrolysis. A particle containing 10 molecules of TG and 40 molecules DG yields the fastest lipid hydrolytic rate of 143 nM FA/h/ $\mu$ M PL, which constitutes 96% DG hydrolysis, 3% TG hydrolysis and 1% PC hydrolysis.

In summary, DG causes specific conformational changes to apoA-I that give rise to a decrease in the particle surface potential and increase in stability. Together, these structural changes appear to regulate the actions of HL; HDL-DG content regulates the hydrolysis of PL, DG and TG by HL. The data indicates that hepatic lipase acts primarily as a surface lipid lipase with HDL particles and that DG is the preferred substrate of HL in HDL.

## DEDICATION

I would like to dedicate this work to my family.

## ACKNOWLEDGEMENTS

I would like to thank everyone who has contributed to the successful completion of this study. In particular, Dr. Daniel Sparks, Tracey Neville, Errol Camlioglu, Tanya Ramsamy and Darren Hutt. Barbara Helliwell deserves a thank you for inspiring me to write. I would also like to express my gratitude to the Medical Research Council of Canada for financial support during my studies.

Finally, I would like to give special thanks to Philip Links for his enduring patience and for asking me what I wanted to accomplish in graduate school.

## TABLE OF CONTENTS

ABSTRACT	ii
DEDICATION	iv
ACKNOWLEDGEMENTS	v
TABLE OF CONTENTS	vi
LIST OF TABLES	ix
LIST OF FIGURES	x
ABBREVIATIONS	xii
INTRODUCTION	
Atherosclerosis	1
Lipoproteins	2
HDL metabolism	4
Hypertriglyceridemia	9
Hepatic lipase	11
ApoA-I conformation in HDL	15
Reconstituted HDL	20
Rationale	22
EXPERIMENTAL PROCEDURES	
Materials	23
Isolation and labeling of HDL	23
Quantification of neutral acylated glycerols	24

Preparation and characterization of reconstituted Lp2A-I complexes	25
Circular Dichroism	26
Radioimmunoassay	27
Purification and assay of HL activity	27
Preparation of [ <sup>14</sup> C]-diolein	28
Substrate incubations with hepatic lipase	29
<b>RESULTS</b>	
Section I: HDL structural analysis	
Characterization of the size and composition of Lp2A-I and native HDL particles	30
Effect of Lp2A-I core composition on the net charge of apoA-I.	33
Effect of Lp2A-I neutral glyceride composition on the secondary structure of apoA-I in Lp2A-I	36
Isothermal denaturation of apoA-I in Lp2A-I.	36
Effect of neutral glyceride content on the immunoreactivity of apoA-I	39
Section II: HDL and hepatic lipase	
Purification of human hepatic lipase	46
Lipid hydrolysis in native HDL by hepatic lipase	46
Effect of HDL surface lipids on lipid hydrolysis by hepatic lipase	52
Effect of Lp2A-I triacylglycerol content on hepatic lipase activity	54

Effect of Lp2A-I diacylglycerol content on hepatic lipase activity	59
DISCUSSION	
Section I: HDL composition and structure	61
Section II: HDL and hepatic lipase	68
Section III: Physiological relevance	75
Section IV: Future experiments	77
REFERENCES	78

## LIST OF TABLES

Table 1.	HDL subfractionation by different techniques	7
Table 2.	Epitope locations on apoA-I of a panel of monoclonal antibodies	18
Table 3.	Compositional and physical parameters of various Lp2A-I	32
Table 4.	Molecular composition of native HDL particles	32
Table 5.	Effect of Lp2A-I lipid composition on the diacylglycerol, triacylglycerol and phospholipid hydrolytic activities of human hepatic lipase	55

## LIST OF FIGURES

Figure 1.	The proposed interfacial mechanism of action of hepatic lipase as an acylglycerol hydrolase.	6
Figure 2.	Contribution of hepatic lipase in HDL conversions.	14
Figure 3.	Primary amino acid sequence and predicted secondary structure of apoA-I.	19
Figure 4.	Reconstituted spherical Lp2A-I subjected to electrophoresis in 8-25% nondenaturing gradient gels	31
Figure 5.	Effect of Lp2A-I glyceride composition on apoA-I net negative charge	34
Figure 6.	Effect of Lp2A-I lipid composition on apoA-I $\alpha$ -helix content	35
Figure 7.	Effect of Lp2A-I glyceride content on the molar ellipticity of apoA-I as measured by GdnHCl denaturation	37
Figure 8.	The free energies of denaturation at zero GdnHCl concentration ( $\Delta G_D^0$ ) for various Lp2A-I particles	38
Figure 9.	Linear epitope map of apolipoprotein A-I	40
Figure 10.	Effect of Lp2A-I glyceride content on apoA-I immunoreactivity as measured by competitive radioimmunoassay (RIA)	41
Figure 11.	Effect of Lp2A-I glyceride content on the availability of apoA-I epitopes between the N-terminus and the central domain	43
Figure 12.	Effect of Lp2A-I glyceride content on the availability of apoA-I epitopes between the central domain and the C-terminus	44
Figure 13.	Purification of human hepatic lipase	47

Figure 14.	Hepatic lipase total hydrolytic activities with native lipoproteins isolated from hyper- and normolipidemic subjects	48
Figure 15.	Hepatic lipase total and triacylglycerol hydrolytic activities with HDL <sub>2</sub> isolated from hypertriglyceridemic and normolipidemic subjects	50
Figure 16.	The hydrolysis of polar and nonpolar lipids in native HDL <sub>3</sub> by HL	51
Figure 17.	The effect of surface lipids on hepatic lipase total and triacylglycerol hydrolytic activities	53
Figure 18.	Effect of the triacylglycerol content of spherical Lp2A-I on HL activation	56
Figure 19.	Effect of the diacylglycerol content of spherical Lp2A-I on HL activation	58

## ABBREVIATIONS

apo	apolipoprotein or apoprotein
CAD	coronary artery disease
CE	cholesteryl ester
CETP	cholesteryl ester transfer protein
Chol	cholesterol
DG	diacylglycerol
FC	free or unesterified cholesterol
FFA	free fatty acid
GdnHCl	guanidine hydrochloride
GGE	gradient gel electrophoresis
HDL	high density lipoprotein
HL	hepatic lipase
HyperTG	hypertriglyceridemic or hypertriglyceridemia
IDL	intermediate density lipoprotein
LCAT	lecithin:cholesterol acyltransferase
LDL	low density lipoprotein
Lp2A-I	reconstituted particles containing two molecules of apoA-I
LPL	lipoprotein lipase
MG	monoacylglycerol
MGAT	monoacylglycerol acyltransferase
NAG	neutral acylated glycerols

PA	phosphatidic acid
PAGE	polyacrylamide gel electrophoresis
PC	phosphatidylcholine
PE	phosphatidylethanolamine
PG	phosphatidylglycerol
PI	phosphatidylinositol
PL	phospholipid
POPC	palmitoyl-oleoyl phosphatidylcholine
PS	phosphatidylserine
RCT	reverse cholesterol transport
SDS	sodium dodecylsulphate
TG	triacylglycerol
TLC	thin layer chromatography
TRL	triacylglycerol-rich lipoproteins
VHDL	very high density lipoprotein
VLDL	very low density lipoprotein

## INTRODUCTION

### *Atherosclerosis*

Atherosclerotic cardiovascular disease is the major cause of mortality in a large segment of the world's population (1, 2). Atherosclerosis can be characterized by the progressive accumulation of cellular and extracellular substances within the lumen of blood vessels until occlusion occurs (1, 2). Lesions, that tend to form at the branch points of arterial blood vessels, advance through three stages (1, 2). The first stage is the fatty streak lesion, at which point lipid-filled macrophages (foam cells) can be found in the subendothelial space. The second is a fibrous plaque, which consists of a core of lipid, derived from necrotic foam cells, and a fibrous cap containing smooth muscle cells and collagen. The final stage is a complex lesion, including thrombus formation and accumulation of fibrin and platelets (1, 2). Once blood vessels become occluded by these plaques, oxygen supply to surrounding tissues is compromised and ischemia results. Even though atherosclerosis can occur throughout the body, the most severe consequences result from strokes or myocardial ischemia (3). If there is insufficient blood flow to maintain aerobic metabolism in the heart muscle, acute cardiac failure may occur (3).

The pathogenesis of atherosclerosis is extremely complex so there are many high-risk factors associated with the incidence of this disease. Genetic predisposition, obesity, advanced age, smoking, hypertension, diabetes mellitus, lack of exercise, nervous tension, and excess plasma levels of cholesterol have been correlated with coronary artery disease (1-3). A strong inverse relationship, however, has been found between

atherosclerosis and plasma levels of high density lipoproteins (HDL) (1-5). It still remains to be fully elucidated how HDL can offer this “protection”. The higher the HDL-cholesterol concentration in relation to the total plasma cholesterol levels, the lower the risk of vascular lipid accumulation (1-5). Even though its cholesterol content is used predominately to estimate HDL plasma levels (5), it is important to understand how all HDL lipid and apoprotein components influence the synthesis, modification and catabolism of this lipoprotein to obtain a clearer idea of HDL’s role in atherosclerosis. Diminished plasma levels of HDL cholesterol are statistically and clinically associated with raised triacylglycerol (TG) levels and potentially proatherogenic disorders of TG-rich lipoproteins (TRL) (6,7). The lipolytic enzyme hepatic lipase (HL) is shown to hydrolyze preferentially TG-enriched HDL and consequently the HL activity is inversely correlated with HDL levels (8,9). The factors responsible for the increased HL activity, however, are unclear. By varying the composition of neutral acylated glycerols (di- and triacylglycerols) of HDL, we have found that the substrate specificity and catalytic regulation of HL are influenced by the remodeling of this lipoprotein.

### *Lipoproteins*

Lipoproteins are mixtures of lipids and specific proteins called apolipoproteins or apoproteins (apo). The physical interactions between these two components allow for the otherwise insoluble lipids to be transported through the aqueous environment of the vascular system. Lipoprotein particles tend to have a common structure with the most insoluble lipids (TG and cholesteryl esters) forming a core that is surrounded by a surface monolayer of amphipathic lipids (phospholipids and unesterified cholesterol) and specific

apoproteins (reviewed in 10). The major categories of lipoproteins are typically classified by their hydrated densities. Chylomicrons (chylol,  $\rho < 0.95$  g/ml), the least dense lipoproteins, are produced by intestinal mucosal cells, secreted into the lymph ducts and then released into the plasma within hours of a meal (10). Lipoprotein lipase (LPL), a lipolytic enzyme bound to capillary endothelial cells, hydrolyzes the TG within the circulating chylol. The liberated free fatty acids (FFA) are stored in adipocytes in times of excess food intake. The remnant particle that is produced after hydrolysis is cleared rapidly from the plasma by receptor-mediated uptake in the liver. The remaining lipids delivered to the liver can then be repackaged into lipoproteins for export to the peripheral cells.

In humans, very low density lipoproteins (VLDL,  $\rho = 0.950$ - $1.006$  g/ml) are synthesized in the liver and then secreted into the plasma (10). During circulation throughout the body, this lipoprotein is also acted upon by LPL to produce smaller particles called intermediate density lipoproteins (IDL,  $\rho = 1.006$ - $1.019$  g/ml) (10). IDL can either be removed directly from the plasma by receptor-mediated uptake in the liver or it can be catabolized by LPL and/or HL into low density lipoproteins (LDL,  $\rho = 1.019$ - $1.063$  g/ml) (10). LDL, a cholesteryl ester (CE) enriched lipoprotein, is typically removed from the plasma by the LDL-receptor (10). The main determinant of LDL cholesterol in blood is the activity of LDL receptors on hepatic cell surfaces (11). If the plasma concentration of LDL is too great for efficient removal by the liver, this lipoprotein can become oxidatively modified and rendered unrecognizable by its receptor (10). The formation of foam cells is promoted when this modified LDL is taken up in an unregulated manner by macrophages (1, 2).

Following LPL lipolytic activity, excess surface material from chylos and VLDL, consisting of unesterified cholesterol (FC), phospholipids (PL) and apoC's, become redundant and join the HDL fraction ( $\rho = 1.063-1.21 \text{ g/ml}$ ) (6-10). While catabolism of large TG-carrying lipoproteins appears to be one source of materials for HDL synthesis, the liver and the intestine also contribute to this diverse population of lipoprotein particles (reviewed in 5, 10). Generally, human HDL consists of approximately 50% lipid and 50% protein but can be classified into larger, less dense HDL<sub>2</sub> or smaller, denser HDL<sub>3</sub> (5, 10). These lipoproteins range in size from 7 to 13 nm and can contain any of the following apolipoproteins: apoA-I, apoA-II, apoA-IV, apoC-I, apoC-II, apoC-III, apoD, apoE, apoH and/or apoJ (10). The major apolipoprotein of HDL, apoA-I, is synthesized by the liver and the intestine (10). Of the other two major apolipoproteins, apoA-II is secreted by the liver, whereas apoE is synthesized by the liver and non-hepatic tissues (10). Because apoA-I appears to be secreted without lipid, it is hypothesized that most HDL is formed extracellularly (10).

### *HDL metabolism*

Like most components in metabolism, HDL plasma levels are in a state of dynamic equilibrium, with oscillations due changes in synthetic and catabolic rates. Numerous studies have shown that gene defects resulting in deficiencies in apoA-I can severely reduce or eliminate serum concentrations of HDL cholesterol (5, 12-14). If allelic variations at both the HL and the apolipoprotein AI/III/AIV loci are considered, approximately 50% of the plasma HDL cholesterol levels in normolipidemic humans can be accounted for (13). The variability in HDL levels usually reflects different amounts of

HDL<sub>2</sub> although the major proportion of human HDL is normally present as HDL<sub>3</sub> (5 and Table 1). Even though the pathophysiological relationship remains obscure, low HDL<sub>2</sub> plasma levels may be a stronger risk factor for atherosclerosis than low HDL<sub>3</sub> levels (14,15).

One of the hypotheses suggested for the “protective” nature of HDL is a process called reverse cholesterol transport (RCT) (reviewed in 16). The removal of excess cholesterol from peripheral cells and its delivery to the liver by HDL is termed the direct pathway of RCT (4, 16). The cholesterol can also be removed in an indirect manner if, after efflux from the peripheral cells, it is transferred from HDL to the triglyceride-rich lipoproteins and then is taken up by the liver with these particles (4, 16). The main acceptor of the effluxed cholesterol is nascent or pre $\beta$ <sub>1</sub>-HDL (4, 16 and Figure 1).

Nascent HDL are small, lipid-poor particles with a characteristic pre- $\beta$  electrophoretic migration on an agarose gel (4, 16 and Table 1). As agarose gel electrophoresis of lipoproteins is based primarily on their electronegativity, pre $\beta$ -HDL with a surface potential of -7.0 to -10.5 mV do not migrate as far as  $\alpha$ -HDL particles with a surface potential of -10.5 to -12.5 mV (17, 18). As can be seen in Figure 1, once the pre- $\beta$  HDL has acquired some cholesterol molecules from the peripheral cells, a cascade of larger HDL with  $\alpha$ -migration characteristics is produced through the action of lecithin:cholesterol acyl transferase (LCAT) (16). This enzyme removes a fatty acid from the *sn*-2 position of phospholipids, found in the surface monolayer of both types of HDL, and then esterifies the 3'-hydroxyl residue of cholesterol to catalyze the production of cholesteryl esters (CE) (16). Because CE is poorly soluble in an aqueous environment, this lipid is shielded by the amphipathic PL and FC, forming a non-polar core in the HDL

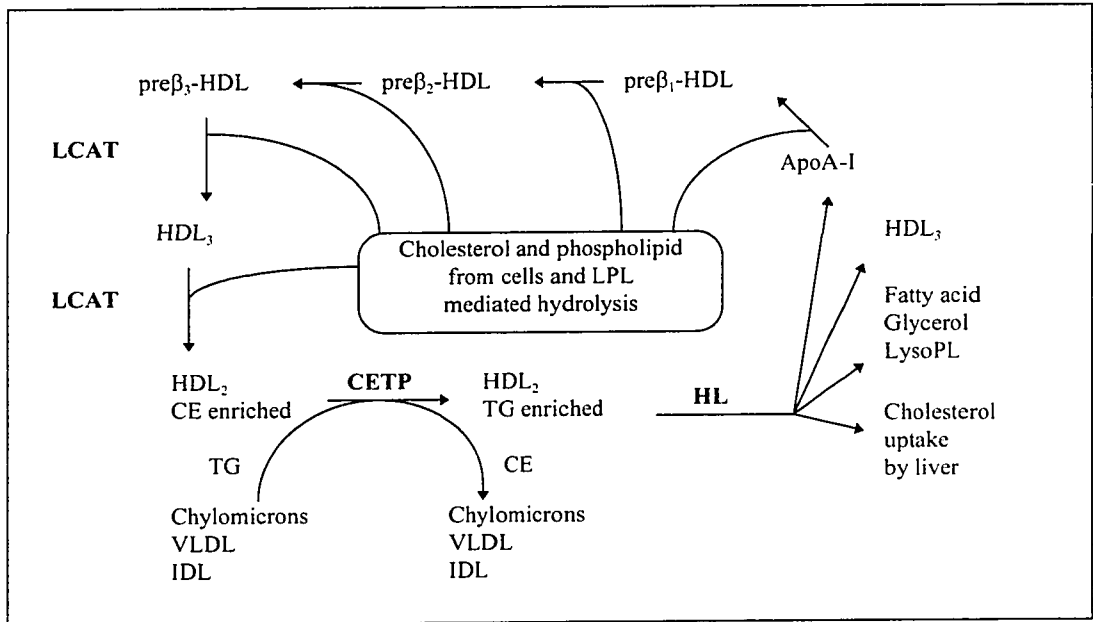


**Figure 1.** Contribution of hepatic lipase in HDL conversions. The apoA-I released from HDL<sub>2</sub> upon hydrolysis of core TG acquires PL and cholesterol from membranes and from surface remnants arising from VLDL and chylomicron hydrolysis. LCAT transfers the *sn*-2 fatty acid of PL to cholesterol generating CE and lysophospholipids. This leads to the formation of larger HDL. CETP stimulates the exchange of CE in HDL for TG from chylom and VLDL. HL mediates the generation of apoA-I and the unloading of HDL cholesterol to hepatocyte plasma membranes. Adapted from Bensadoun and Berryman (19).

**Table 1.** HDL subfractionation by different techniques

a) sequential ultracentrifugation (20, 21)						
Subfraction	VHDL <sub>2</sub>	VHDL <sub>1</sub>	HDL <sub>3</sub>	HDL <sub>2</sub>	HDL <sub>1</sub>	
Density (g/ml)	>1.250	1.210-1.250	1.125-1.210	1.063-1.125	1.055-1.063	
Protein:lipid ratio	97:3	65:35	55:45	40:60		
b) polyacrylamide gradient gel electrophoresis (22, 23)						
Subfraction	HDL <sub>3c</sub>	HDL <sub>3b</sub>	HDL <sub>3a</sub>	HDL <sub>2a</sub>	HDL <sub>2b</sub>	HDL <sub>1</sub>
Density (g/ml)	1.167-1.200	1.147-1.167	1.125-1.147	1.100-1.250	1.063-1.100	1.055-1.063
Stokes' diameter (nm)	7.8	8.4	9.0	9.6	10.8	12.0
Relative cholesterol content (%)						
Men	4	17	35	22	21	1
Women	4	11	32	21	31	1
c) two dimensional agarose and polyacrylamide gel electrophoresis (16, 17)						
The majority of plasma HDL (95-98%) is comprised of $\alpha$ -migrating particles. An $\alpha$ -migration corresponds to a surface potential of -10.5 to -12.5 mV. However, 2-5% of plasma HDL has a pre $\beta$ -migration and size of 5-6 nm. Ranging from the smallest to largest in size, these particles are termed pre $\beta$ <sub>1</sub> -, pre $\beta$ <sub>2</sub> - and pre $\beta$ <sub>3</sub> -HDL, respectively. A pre $\beta$ -migration corresponds to a surface potential of -7.0 to -10.5 mV.						

particle. Different subfractions of HDL (Table 1) are then generated as the core increases in size, varying from VHDL to HDL<sub>3</sub> to HDL<sub>2</sub> (smallest to largest  $\alpha$ -HDL) (4, 16).

Most of the CE does not remain in the HDL pool but is transferred to VLDL, IDL and LDL through the action of cholesteryl ester transfer protein (CETP) (16 and Figure 1). The removal of CE from HDL may be accompanied by a reciprocal transfer of TG from TRL into HDL and lead to further remodeling of this lipoprotein (16). TG-enriched HDL<sub>2</sub> is thought to be a good substrate for HL as studies have shown that HDL<sub>2</sub> levels

are reduced, while HDL<sub>3</sub> plasma levels are enhanced, with increased activity of this enzyme in hypertriglyceridemic (hyperTG) patients (8). Investigations by Patsch *et al.* (8, 9) have shown that changes in HDL subclass size distribution are closely associated with an abnormal TG metabolism.

Catabolism of HDL is not well understood (24). On the basis of the observations that the various HDL components turn over at different rates, catabolism is thought to involve partly the clearance of HDL lipid by selective uptake in the liver and steroidogenic tissues (25). HDL binds to the cell surface, transfers its CE, to the cell and the lipid-depleted HDL is released into the extracellular fluid (25). HL and the scavenger receptor B-1 (SR-B1) may be acting in concert during selective HDL-CE uptake. HL is found preferentially in tissues that express high levels of SR-B1. Thus, HL and SR-B1 have been implicated in the selective uptake process (26). As the hydrophobic CE resides in the core of the lipoproteins, it may be necessary for the outer membrane's integrity to be disrupted by HL (27) and then these HL-digested particles may be better able to transfer their core lipids to the cells via an SR-B1 mediated mechanism (26). The work of Kadowaki *et al.* (27) has demonstrated that HL-mediated PL hydrolysis promotes the uptake of HDL-derived cholesteryl ester by the rat liver. This group found that if a nonhydrolyzable PC analogue is used, there is very little uptake of cholesteryl oleate.

Hepatic uptake of HDL-PL was found to be dependent on the nature of the polar head group, but was not related to the HL-mediated PL or TG hydrolysis, based on perfused rat liver experiments (28). While TG hydrolysis resulted in rapid transfer of the liberated FFA into the liver with no other detectable neutral acylated glycerols (NAG) in the perfusate, lysophospholipids were found associated with albumin (28). Any PL

uptake appears to take place by the transfer of intact molecules between HDL and liver cells through either an exchange or net uptake (28). Barrans *et al.* (29) found that the formation of pre $\beta$ -HDL, or lipid-poor apoA-I, is increased in the presence of HL in a perfused rat liver system, indicating that non-hydrolyzed PL may get recycled with the apoA-I back into circulation. This lipid-poor particle can then be involved in cholesterol efflux or removed by the kidney (30).

In addition to the uptake of lipid by the liver, HL appears to be involved in the clearance of apoA-I from the plasma. The hydrolysis of TG-enriched HDL<sub>2</sub> by this enzyme promotes the formation of smaller HDL<sub>3</sub> particles and the liberation of free or lipid-poor apoA-I (29-31). This can lead to an increase in renal clearance of apoA-I (30), or a stimulation of cholesterol efflux, or both (16). Under normal circumstances, increased cholesterol efflux would be considered beneficial if the excess cholesterol is eliminated by the body through the liver. Transfer of HDL-CE into the TRL, however, could result in the delivery of some cholesterol back to the peripheral cells. Over time, this could result in accumulation of cholesterol in tissues, including the arterial wall, especially if these lipoproteins become oxidatively modified (4, 16). In most hyperTG patients there is increased HL activity, decreased plasma levels of HDL<sub>2</sub>, elevated levels of small HDL particles and potentially atherogenic accumulation of CE in apoB-containing lipoproteins (6-9).

### *Hypertriglyceridemia*

It is important to preface this section with a statement about the clinical measurements of triacylglycerol. All large-scale studies use techniques that measure all

NAG species yet state these values as the plasma TG levels (32, 33). While there has been some attempt to measure individual glycerol species in normolipidemics (32) and HDL isolated from normolipidemics (33), these measurements have not been performed on hyperTG patients. Thus, all values published for these patients represent the total plasma levels of free glycerol, monoacylglycerols (MG), diacylglycerols (DG) and TG. Terms such as hypertriglyceridemia (hyperTG) and triglyceride plasma levels are used but it should be kept in mind that the other NAG concentrations may also be elevated.

TG plasma levels can range from normal (below 2.2 mmol/L or 200 mg/dL), borderline (2.2 - 4.5 mmol/L) to hyperTG (above 4.5 mmol/L or 400 mg/dL) (7). Elevated plasma TG levels are associated with lower HDL levels, especially HDL<sub>2</sub> (6, 7). HDL particle size distribution is influenced by the transfer of TG and CE between HDL and TRL (34). In hyperTG patients, the residence time of circulating chylos and VLDL is increased and thus the transfer of TG into HDL is enhanced (34). As TG-rich HDL<sub>2</sub> is the preferred substrate for HL, these large particles are hydrolyzed into small, dense HDL (34). Patsch *et al.* (8,9) have postulated that this abnormal HDL profile is in response to low levels of LPL activity, a prolonged postprandial lipemia and high levels of HL activity. The magnitude of postprandial lipemia is determined by a number of factors, including: LPL, HL, apolipoproteins, LDL receptor, LDL receptor-related protein (LRP), age, gender, exercise and insulin levels (35).

Reaven (36) has suggested that delayed removal of chylomicron remnants is part of an atherogenic phenotype called syndrome X. These patients typically present hypertriglyceridemia, low HDL, small dense LDL, insulin resistance and in many cases, mild hypertension with obesity (reviewed in 36). Insulin resistance can lead to

compensatory hyperinsulinemia and then non-insulin-dependent diabetes mellitus (NIDDM or Type 2) (36). Insulin clears fatty acids and glucose from the blood by increasing uptake and storage, and by decreasing mobilization of stored energy within the adipocytes (37). While insulin stimulates LPL activity in normal subjects, in obesity and NIDDM, the response of adipose tissue LPL to insulin is blunted (36-41). With reduced LPL activity, the post-prandial response is prolonged, TRL levels are increased, triglyceride enrichment of HDL<sub>2</sub> increased and HL action stimulated (35). The direct effect of insulin on HL is not well understood but the ratio of HL-to-LPL activity in these patients influences the HDL<sub>2</sub> plasma levels and may be an indicator of their atherosclerotic risk (8, 9, 38, 39)

### *Hepatic lipase*

HL (hepatic triacylglycerol lipase EC 3.1.13) is synthesized and secreted by hepatocytes and then, through an ionic interaction with heparin sulfate proteoglycans, binds to the surface of the endothelium in liver sinusoids (42). The space between the endothelium and the hepatocyte, where HL can be found, is called the Space of Disse (43). Molecules must pass through the fenestrae between the endothelial cells that line the hepatic sinusoids to gain access to this space and to the surface of each hepatocyte (43). In addition to the liver expression of HL, Verhoeven and Jansen (44) found that a truncated HL mRNA exists in ovaries, adrenals and testes which may produce an intracellular form of HL with a unique role in steroidogenic cells.

The human HL gene can be found in band 15q21, is 35 kb long and has 9 exons (45, 46). Mature human HL is a 476-amino acid glycoprotein with a calculated molecular

weight of 53,431. The purified denatured HL has an apparent molecular weight of 65-69,000 reflecting the contribution of N-linked carbohydrates (45-47). The functional unit of HL appears to be a homodimer (47). HL gene expression is sensitive to sex steroids. In humans, androgens up-regulate HL activity, while estrogens down-regulate it (reviewed in 48). This hormonal regulation has been postulated to give rise to the elevated HDL<sub>2</sub> levels and reduced atherosclerotic risk in premenopausal women relative to men (48). Deficiency of HL is characterized by elevated VLDL plasma levels, the presence of  $\beta$ -VLDL and abnormally high TG-rich LDL and HDL (49). Patients with complete HL deficiency have elevated cholesterol and TG levels and some have premature atherosclerosis (49). HL deficiency mimics the Type III hyperlipidemia phenotype so DNA screening would help reveal whether an apoE 2/2 isotype or an HL mutation was responsible for the elevated lipid levels and the diseased state (49).

Targeted inactivation of the mouse HL gene leads to mild dyslipidemia (50). These mice showed increased HDL-PL and cholesterol but unchanged TG levels. They also had increased apoB48 remnants and  $\alpha$ -migrating HDL (50). Overexpression of the human HL gene in cholesterol-fed mice leads to a 34% reduction in plasma HDL-cholesterol levels and a corresponding decrease in total cholesterol and HDL particle size (51). In addition, there was a decrease in the accumulation of aortic cholesterol (51). Since the mouse is predominately an HDL animal and resistant to atherosclerosis, the absence of an atherogenic profile with increased HL needs to be accepted cautiously when drawing parallels to the human condition (51).

The study of lipolytic enzymes has been complicated by differences in the physical states of various lipid substrates (52). It is also difficult to calculate meaningful

Michaelis-Menten  $K_m$  and  $V_{max}$  values due to the interfacial nature of the substrate-enzyme interactions (53). See Figure 2 for the proposed method of HL interaction with lipoproteins. HL hydrolyses the *sn*-1 fatty acyl ester bonds of phospholipids as well as the *sn*-1 (*sn*-3) ester bonds of mono-, di- and triacylglycerols (42). Through the use of mixed micelles, Waite *et al.* (52) determined relative hydrolytic rates for a number of different substrates with rat HL. This group observed that rat HL could hydrolyze phosphatidic acid (PA) > phosphatidylethanolamine (PE) > phosphatidylcholine (PC) > phosphatidylinositol (PI). Via comparison with neutral lipids, they concluded that HL prefers substrates without polar head groups. They could not use TG in their system but MG, 1,2-DG and 1,3-DG were all hydrolyzed at a rate faster than the phospholipids (52).

Waite's group (54) also used a lipid monolayer system to investigate the substrate specificity of human HL. It was assumed that regardless of which lipoprotein particle being the substrate, hydrolysis probably takes place at the monomolecular surface film of lipoproteins (54). Again, TG was found to be a poor substrate on its own and thus required dilution by PL to be actively hydrolyzed. The increased hydrolysis of TG in the presence of PL was not due to increased penetrance by HL through the monolayer (54). The substrate specificity for PL within pure lipid monolayers was found to be slightly different than with the rat HL experiment (51). This time the hydrolytic rates were in the following order: PE > PA > phosphatidylglycerol (PG) > phosphatidylserine (PS) > PC (54). Based on these experiments, the authors concluded that the catalytic activity and the substrate preference of HL is regulated by a complex interplay between physiochemical properties, mainly lipid packing and surface pressure, of the surface lipid film of lipoproteins and the apolipoprotein composition of lipoprotein particles (54).

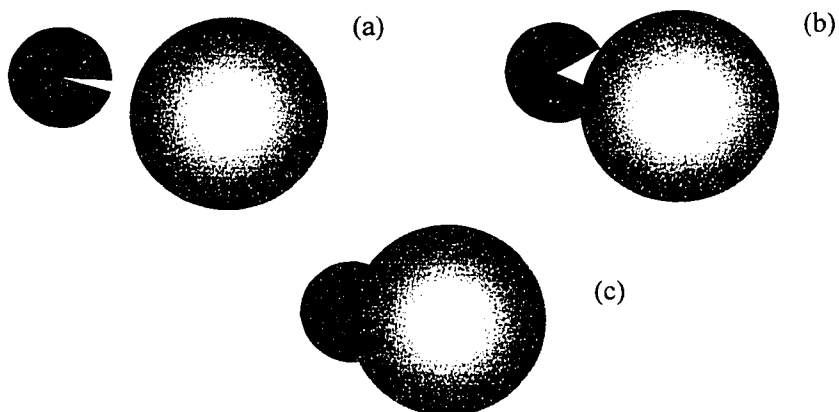


**Figure 2.** The proposed interfacial mechanism of action of hepatic lipase as an acylglycerol hydrolase. (a) Illustrates an HDL particle (grey sphere) in proximity to HL (black semi-circle). The catalytic triad residues are hidden by a conformation-dependent “lid”. The limited access is schematically represented by the small-sized white wedge. The initial interaction of HL with HDL leads to a conformational change and the opening of the HL lid, exposing the non-polar, hydrophobic residues of the HL amphipathic helices (b). The substrate, thus gains access to catalytic site where hydrolysis takes place (c). Adapted from Santamarina-Fojo and Dugi (55).

Analysis of HL activities and the composition of HDL have identified several important relationships. HL appears to be involved in the remodeling of HDL and is capable of converting TG-enriched HDL<sub>2</sub> from postprandial plasma to smaller particles in the HDL<sub>3</sub> density range (8). Following VLDL hydrolysis by LPL, Simard *et al.* (56) incubated the VLDL with HDL. Their data showed that the hydrolysis of HDL-PC by HL was influenced more by changes in the particle's surface rather than the lipid core (56). Following free cholesterol enrichment of native HDL, some of the same investigators (57) observed increased hydrolysis of PE, PC and TG.

### *ApoA-I conformation in HDL*

ApoA-I is an exchangeable apolipoprotein that contains numerous stretches of amphipathic  $\alpha$ -helix within its 243 amino acid length (58). To be defined as amphipathic  $\alpha$ -helices, there needs to be a large nonpolar face that associates with the fatty acyl chains of PL and a polar face in which Asp, Glu, Lys and Arg are typically distributed so that negatively charged residues are at the centre and positively charged residues are at the periphery of the face (58). The gene for apoA-I, as with many other exchangeable apolipoproteins, contains multiple repeats that code for the 11 and 22 amino acid sequences making up amphipathic  $\alpha$ -helices (58). With 3.6 amino acid residues per turn of an  $\alpha$ -helix, 22 residues equal six complete turns (58). Many of the tandem repeats have prolines at the first and only first position (58 and Figure 3). The predicted  $\alpha$ -helical secondary structure, based on hydrophobicity calculations (59), is in strong agreement with the tandem repeats encoded by exon 4 (Figure 3). The hydrophobicity values for a stretch of amino acids indicate what type of secondary structure is most probable. While

it is known that the conformation of apoA-I differs between its lipid-bound and aqueous-soluble forms (60), it remains to be determined if the  $\alpha$ -helices are arranged antiparallel to one another in the presence of lipid (61, 62) and in a continuous horse-shoe-like fashion in the absence of lipid as depicted by the recent x-ray crystal structure (63). Adding to the evidence of apoA-I structural adaptability,  $^{13}\text{C}$ -NMR studies showed that the conformation of apoA-I on discoidal complexes is dependent on particle size and that these conformations are substantially different from that of apoA-I on spherical complexes (62). Due to the differing view points on apoA-I secondary structure, a model depicting apoA-I on the surface of lipoprotein has not been included.

Alterations in HDL composition give rise to specific changes in the charge, conformation and stability of apoA-I, as measured by agarose gel electrophoresis and isothermal denaturations. In the absence of lipid, apoA-I has a measured surface charge of -8.3 mV, an  $\alpha$ -helix content of 46% and a thermal stability ( $\Delta G_D^\circ$ ) of 2.4 kcal/mol (64). In the presence of 70 molecules of POPC, the charge decreases to -9.3 mV, the  $\alpha$ -helical content raises to 58%, and the stability decreases to 1.2 kcal/mol apoA-I (65). Inclusion of either CE or TG in spherical LpA-I increases both the  $\alpha$ -helix content and stability, while the surface charge becomes more negative (65). Interestingly, increasing the TG:CE ratio in spherical LpA-I containing both neutral lipids diminishes the stability of the  $\alpha$ -helical segments of apoA-I (65). Sparks *et al.* (65) suggest that this decreased stability could lead to the dissociation of apoA-I from HDL in the hyperTG state where a high TG:CE ratio exists and the plasma concentration of lipid-poor or free apoA-I (pre $\beta$ -HDL) is elevated (66).

Typically, the lipid composition of HDL has been expressed in terms of FC, PL and TG. However, recent observations of Vieu *et al.* (33) have shown that the methods used to measure TG have masked the contributions of DG in this lipoprotein class. Their study showed that most of the NAG in HDL are DG and that the DG:TG ratio in HDL can be up to 7:1. Because HDL lipid composition can have major effects on the structure and function of this lipoprotein (64, 67, 68), it is conceivable that DG may affect the conformation of the main apolipoprotein in HDL, apoA-I and also affect the interactions between HL and HDL particles.

Secondary and tertiary conformational changes of apoA-I, brought about by altered lipid compositions, have also been studied in the lab of Marcel and colleagues (61, 68-70). Monoclonal antibodies (mAb) represent sensitive probes with which to study the structure and function of apoA-I as most mAbs raised against lipoproteins recognize conformational epitopes (60). The authors studied five domains within apoA-I and observed that various regions of the molecule respond differently to changes in the phospholipid and cholesterol concentrations (68-70). Listed in Table 2 are the residues of apoA-I within native HDL and discoidal LpA-I that are immunoreactive with a panel of monoclonal antibodies and the estimated exposure of these domains with increases in PL or FC. Their studies indicate that apoA-I is a flexible protein that can respond to specific constituents and their concentration in the lipid milieu of an HDL particle (68-70).

Other investigations with mAbs against apoA-I have looked at various structure function relationships for this protein. Banka *et al.* (71) found that mAbs blocking the central region of apoA-I could reduce LCAT activation by up to 80%, while Meng *et al.* (72) observed that specific N-terminal and central domains (4H1 and A11) mAbs

**Table 2.** Epitope locations on apoA-I of a panel of monoclonal antibodies as determined by Marcel *et al.* (61). Immunoreactivity is shown in the presence of increased phospholipid (PL) or free cholesterol (FC) concentrations for native HDL (68) and for discoidal LpA-I (69). ↑ indicates that the domain is more exposed, ↓ is less exposed, -- represents no change, h is a heterogeneous response and a blank space indicates not measured.

Antibody	Epitope location (residues of apoA-I)	Immunoreactivity			
		Native HDL		Discoidal LpA-I	
		↑ PL	↑ FC	↑ PL	↑ FC
4H1	2-8	--	↑	↓	↑
2G11	44-50, 58-64, 77-82, 96-112	↓	--	↑	--
A51	23-29, 60-82			↑	--
A05	25-82			↑	--
A17	98-112				
A11	99-105, 126-132			↓	↑
A44	149-186			h	--
4A12	173-205	--	↓	h	--

stimulated cholesterol esterification. Fielding and Fielding (16) have proposed that residues 143-165 of apoA-I interact with LCAT and Sparks *et al.* (73) further suggested that conformational changes to residues 100-122 may regulate this interaction. Other work has focused on different functions of apoA-I. Fielding *et al.* (74) found that within pre $\beta_1$ -HDL, residues 137-144 of apoA-I may be important for cholesterol efflux. A putative cholesterol binding domain has been identified within residues 100-122 (75). Frank *et al.* (70) have found that if the central helices of apoA-I are deleted, there is decreased binding to phospholipids. Future mAbs studies with mouse SR-B1 and its human equivalent, Cla-1 should prove interesting as these proteins are putative HDL binding sites on steroidogenic tissues (26).

1. DEPPQSPWDRVKDLATVYVDVLKDSGRDYVSQFEGSALGKQLNLKLLDNW

◆-----◆-----◆-----◆◆-----  
ccccccccccccccccccccchhhhhhhhhcc

51. DSVTSTFSKLREQLGPVTQEFWDNLEKETEGLRQEMSKDLEEVKAKVQPY

-----●-----●-----  
ccccchhhhhhhccchhhhhhhhhhhhhhhhhhhhhhhhhhhhhhh

101. LDDFQKKWQEEMELYRQKVEPLRAELQEGARQKLHELQEKLSPLGEEMRD

-----●-----●-----  
hhccchhh

151. RARAHVDALRTHLAPYSDELQRLAARLEALKENGGARLAEYHAKATEHL

-----●-----●-----  
hhhhhhhhhhhhccchhhhhhhhhhhhhhhccchhhhhhhhhhhhh

201. STLSEKAKPALEDLRQGLLPVLESFKVSFLSALEEYTKKLNTQ

-----●-----●-----  
hhhhhhhhhhhhhhhhccchhhhhhhhhhhhhcc

**Figure 3:** Primary amino acid sequence and predicted secondary structure of apoA-I. Upper case letters represent the single-letter code for the amino acids. The basic or positively charged amino acids, lysine (K), arginine (R), and histidine (H) are shown in blue. The acidic or negatively charged amino acids, aspartic acid (D) and glutamic acid (E) are shown in red. Proline (P) is shown in green. Below each string of amino acids, ◆---◆ represents an 11-mer encoded by exon 3, while ●---● represents either an 11-mer or a 22-mer tandem repeat encoded by exon 4. Lower case “c” indicates a predicted coiled region, while “e” is extended and “h” is  $\alpha$ -helix.

## *Reconstituted HDL*

Structure and function studies of native HDL particles have been hampered by their biological heterogeneity and by technical limitations that have made isolation of monodisperse LpA-I or LpA-I,A-II populations very difficult. Investigation of molecular details of the structure/function relationships involved in HDL metabolism requires the use of well-defined, homogeneous substrates. It is implicit that to define the physical structure and function of a molecule, all molecules in a preparation should be as similar as possible. To accomplish this goal, some investigators have utilized homogeneous reconstituted LpA-I complexes for structure/function studies. The most commonly characterized of these reconstituted preparations are simple phospholipid-apolipoprotein mixtures that form disc-shaped particles. Discoidal LpA-I are generally produced by cholate-phospholipid dispersion methods (reviewed in 76) and since highly homogeneous populations can be produced, these systems have been thoroughly studied in terms of their biophysical and metabolic characteristics (76-78). While these simple systems differ substantially from the mature spherical LpA-I particles of the plasma, which contain a neutral lipid core, they appear to resemble more closely nascent HDL particles found in the interstitial fluid (79). Discoidal particles have been the preferred models for the study of lipid-protein interactions (69, 76-78) and also for LCAT substrate specificity (73, 80). Investigators have utilized a wide variety of biophysical techniques to elucidate the conformation of apoA-I in discoidal particles, however, the elucidation of apoA-I conformation in spherical particles has only recently become feasible.

The reason spherical HDL particles have been studied to a lesser extent is that the

techniques used for their production tend to generate very heterogeneous preparations and are often not reproducible (76). In the seventies, Ritter and Scanu (81) showed that reconstituted spherical LpA-I,A-II particles could be produced from repurified lipids and apoproteins by co-sonication. Investigations have since shown that reconstituted spherical LpA-I,A-II resemble authentic HDL in their ability to interact with LCAT and CETP (82, 83), lipoprotein lipase (84) and cultured cells (85). While spherical reconstituted lipoproteins are much more comparable to the HDL found in plasma, size characteristics have shown these preparations to be as heterogeneous as their native HDL counterparts. The structural heterogeneity has limited the characterization of the molecular and functional properties of spherical particles. To overcome this limitation, Sparks *et al.* (65) have developed a novel sonication technique to produce highly homogeneous spherical LpA-I and LpA-I,A-II. It is now possible to clearly demonstrate how the structural remodeling of HDL affects this lipoprotein through the production and study of these mono-disperse populations of particles.

In recent studies with homogeneous spherical LpA-I, Sparks *et al.* (64) showed that the overall conformation of apoA-I is significantly different in spherical particles containing a CE core, than in discoidal complexes. These studies also showed that the surface charge and secondary structure of apoA-I are significantly different on spherical particles and appear to be modulated by changes in complex composition in an entirely different manner than for apoA-I on discoidal LpA-I particles (64). In addition, studies with increased TG:CE ratios showed decreased stability of the lipoprotein particles (65). HDL particles found in the plasma of hyperTG subjects are increased in TG and depleted of CE (34, 86) so it is possible that the unusual charge and structural characteristics of TG-rich HDL may give rise to differences in the functional properties of these lipoproteins. Because the total NAG are

measured when plasma TG levels are determined (31, 32), it is also possible that free glycerol, MG or DG plays an important role in the metabolism of HDL.

### *Rationale and objectives*

The inverse relationship between HDL and atherosclerosis has led to an intense investigation into the metabolism of this lipoprotein. Because of the strong inverse relationship between HDL<sub>2</sub> plasma levels and HL activity (8, 13, 35, 39), an understanding of the factors involved in the catalytic regulation of this enzyme is crucial to the understanding of the role HL plays in atherosclerosis. Unfortunately, the heterogeneous nature of native lipoproteins can confound estimations of what may be influencing the activity or substrate specificity of HL. The use of a well-defined reconstituted HDL model, however, provides an ideal tool by which one experimental variable can be altered at a time. In this way, the effects of DG and TG on the charge, stability and conformation of apoA-I and the reactivity of HL can be tested. In this investigation it will be shown that homogeneous reconstituted HDL particles are good lipoprotein analogues to study the structural effects that DG has on apoA-I charge, stability and conformation. In addition, it will be shown that Lp2A-I particles are good models to study HL-mediated lipolysis and that the DG content of Lp2A-I greatly affects the ability of human HL to hydrolyze HDL lipids. Finally, it will be demonstrated that there is a correlation between HDL structural properties and the hydrolysis of this lipoprotein by HL.

## EXPERIMENTAL PROCEDURES

### **Materials**

Triolein (TG), unesterified cholesterol (FC) and phospholipase C (Type I from *C. perfringens*) were purchased from Sigma Chemical Co. (St. Louis, MO) while 1,3-diolein (DG) and fatty acid standards were acquired from NuChek Prep., Inc. (Elysian, MN). Palmitoyloleoyl phosphatidylcholine (POPC), sphingomyelin (SPM) and phosphatidylinositol (PI) were obtained from Avanti Polar Lipids (Birmingham, AL). Tri[9,10-<sup>3</sup>H(N)]olein was purchased from DuPont Canada Inc. (Mississauga, ON), while di[1-<sup>14</sup>C]oleoyl phosphatidylcholine was obtained from Amersham Canada (Oakville, ON). All other reagents were analytical grade. The polyclonal antibody against HL was a generous gift from Dr. Howard Wong at the University of West LA, Department of Veterans Affairs Medical Center, Los Angeles, California. The monoclonal antibodies (mAbs) against apoA-I were a generous gift from Dr. Yves Marcel, University of Ottawa Heart Institute, Ottawa, Ontario.

### **Methods**

**Isolation and labeling of HDL.** Subfractions of HDL were obtained from plasma by density gradient ultracentrifugation as described by Guérin *et al.* (87). The density gradient was established between 1.006 g/ml and 1.24 g/ml and then the samples were centrifuged at 40,000 rpm at 4°C for 20 hours. 13 different fractions were obtained with HDL<sub>2</sub> in fractions 8 and 9 and HDL<sub>3</sub> in fractions 10 and 11. Incorporation of [<sup>3</sup>H]-triolein and [<sup>14</sup>C]-diolein (preparation described below) into HDL was accomplished by incubation of POPC vesicles containing the labeled lipids (65, 88). PL, TG and DG vesicles were prepared, by drying 50 µg of POPC, 100 000 cpm of [<sup>3</sup>H]-triolein and 50

000 cpm of [<sup>14</sup>C]-diolein under N<sub>2</sub>, addition of 200 µl of 10 mM phosphate-buffered saline (PBS), pH 7.2 and vortexing for one minute. Vesicles were combined with HDL<sub>2</sub> or HDL<sub>3</sub> (2 mg of protein) and incubated with gentle shaking for 8 hours at 37°C. Greater than 95% of the radioactive lipids were incorporated into the HDL particle after reisolation. HDL lipid mass values were determined as described below and the lipid specific activities were calculated.

To incorporate additional surface lipids into HDL, a procedure involving Celite incubation was adapted from Sparks *et al.* (88). SPM, PI or FC (4 mg) was added to 50 mg of Celite (diatomaceous earth) and then dried under N<sub>2</sub>. Enough 10 mM PBS, pH 7.2 was added to bring the volume to 2 ml in the presence of HDL<sub>3</sub> (2 mg). The mixture was incubated overnight with gentle shaking at 37°C. After transferring to Eppendorf tubes and centrifuging at 14 000 rpm for 10 minutes, the supernatant was isolated.

***Quantification of neutral acylated glycerols.*** HDL lipids (per 1 mg protein) were extracted by the method of Bligh and Dyer after the addition of 12 µl of formic acid per ml of aqueous phase (33). Before extraction, internal standards of [<sup>14</sup>C]-diolein and [<sup>3</sup>H]-triolein (15,000 cpm each) were added to the tubes. The organic phase was removed, evaporated under nitrogen to dryness and redissolved in 50 µl chloroform. Thin layer chromatography on silica gel 60 plates, using a solvent system of hexane:diethyl ether:acetic acid (105:45:1.5, v/v), was undertaken to separate the glycerol-containing neutral lipids. The following R<sub>f</sub> values were obtained: MG = 0.01, 1,2-DG = 0.08, 1,3-DG = 0.14 and TG = 0.53. The spots corresponding to DG and TG were scraped into 1.5 ml Eppendorf tubes and 100 µl of isopropanol plus 500 µl of the enzyme solution from the Boehringer Mannheim TG kit (Cat. No. 701 882) was added. The samples were

incubated at room temperature overnight and then 200  $\mu$ l aliquots of the supernatant were spectroscopically analyzed to determine glycerol content. Through the use of diolein and triolein standards, it was determined that the enzyme reaction was able to go to completion within the given time period. MG was not measured quantitatively due to the presence of glycerol at the origin of the plate.

***Preparation and characterization of reconstituted Lp2A-I complexes.*** Purified apoA-I was isolated from delipidated HDL by size exclusion chromatography (72, 89) and spherical reconstituted Lp2A-I were prepared by co-sonication of POPC, triolein, diolein and apoA-I as previously described (65). POPC (3.2 mg) and other purified lipids in chloroform (see Table 3 for starting concentrations) were dried under nitrogen into a 12 x 75 mm test-tube and 800  $\mu$ l of phosphate/saline pH 7.4 was added. The lipid-buffer solution was initially sonicated for 1 min in a 15°C water bath and under nitrogen using a Branson 450 sonicator with 1/8" tapered microtip probe. The suspension was then incubated in a sealed tube for 30 min at 37°C and sonicated again for 5 min using a 95% duty cycle. Apo A-I (3 mg of a 1.8 mg protein/ml phosphate/saline solution, pH 7.4) was added to the lipid suspension and the protein-lipid mixture was sonicated for 4 x 1 min punctuated by 1 min cooling periods. All Lp2A-I complexes were filtered through a 0.22  $\mu$ m syringe tip filter and reisolated by size exclusion chromatography on a Superose 6 column.

The size and homogeneity of apoA-I complexes were estimated by non-denaturing gradient gel electrophoresis on precast 8-25% acrylamide gels (Pharmacia Phastgel) after protein staining and densitometric scanning. Lipoprotein particle mobility, valence and surface charge characteristics were determined by electrophoresis on precast

0.5% agarose gels (Beckman, Paragon kits) (17, 18). The agarose electrophoretic mobility was obtained by dividing the electrophoretic velocity (migration distance/time) of the lipoprotein particle by the electrophoretic potential (voltage applied/gel distance). From this value, the net charge or valence of the particle was derived (17, 18). Proteins were determined by the Lowry method as modified by Markwell *et al.* (90). NAG, fatty acids and phospholipids were determined enzymatically using Boehringer Mannheim kits. Sphingomyelin was measured enzymatically using the PC kit after separation of the phospholipids by TLC on a silica gel K6 plate with chloroform:methanol:acetic acid:H<sub>2</sub>O (25:15:4:2, v/v) for a mobile phase. Phosphatidylinositol content was determined as the difference between the PC content (enzymatic measurement) and the total phospholipid content, measured by the method of Sokoloff and Rothblatt (91).

**Circular Dichroism.** The average secondary structures of Lp2A-I apoA-I were monitored by circular dichroism spectroscopy using a Jasco J40A spectropolarimeter (64). The percent  $\alpha$ -helix in apoA-I was calculated from the molar ellipticities at 222nm ( $\theta_{222nm}$ ) using a mean residue weight of 115.3. The effect of GdnHCl concentration on the secondary structure of apoA-I in various Lp2A-I particles was monitored by the changes in molar ellipticities. Circular dichroic absorbances at 222 nm were converted to molar ellipticities over a range of GdnHCl. The free energy of unfolding of apoA-I on the surface of Lp2A-I complexes ( $\Delta G_D^\circ$ ) was calculated according to the following equation:

$$\Delta G_D^\circ = \Delta G_D + \Delta n \times RT \ln(1 + ka), \text{ where}$$

$\Delta G_D^\circ$  = the standard free energy of denaturation at zero GdnHCl concentration

$\Delta G_D$  = the standard free energy of denaturation

$\Delta n$  = the difference in the moles of GdnHCl bound by the protein  
in the native and denatured states

R = the gas constant (1.98 cal/K)  
T = the temperature in degrees K  
k = the average association constant of GdnHCl and protein  
a = the mean ionic activities of GdnHCl

**Radioimmunoassay.** The conformation of apoA-I on the different Lp2A-I was evaluated from the immunoreactivity of a panel of mAbs against apoA-I (68). Apo-HDL was incubated overnight in Remova wells at 4°C and then the non-specific sites were blocked with gelatin. Appropriate dilutions of the antigen (Lp2A-I particles) and the series of mAbs were co-incubated in microtitre wells and then transferred into the remova wells for an incubation time of 1 h. The amount of antibody remaining in the well was detected by a secondary anti-mouse antibody labeled with <sup>125</sup>I. ED<sub>50</sub> values, the antigen concentrations at which half maximum binding of the antibody were attained, were calculated from the slope of the linear portion of a plot of B/B<sub>0</sub> versus the log of antigen concentration. B/B<sub>0</sub> refers to the amount of counts bound compared to the maximum amount of counts that could be bound.

**Purification and assay of hepatic lipase activity.** HL was purified from post-heparin human plasma by heparin affinity chromatography as described by Ehnholm and Kuusi (92). After post-heparin human plasma was collected from normolipidemic subjects, a 20 % TG emulsion (LIPOSYN II, Abbott Laboratories, Ltd., Montréal, PQ) was added to the plasma and the resulting cakes of fat were harvested for delipidation. The resuspended, aqueous solution of crude HL was loaded on to a heparin-sepharose CL-6B column and eluted with a linear salt gradient of 0.15M to 1.5M NaCl in 5 mM sodium barbital, pH 7.4, 20% glycerol. HL activity was characterized using a standard particle containing a neutral lipid core (POPC: TG: apoA-I of 120:20:2, mol/mol/mol),

quantified into units of enzyme activity (where 1 unit = 1 nmol fatty acid hydrolyzed/mg protein/h from a 120:20:2 POPC:TG:apoA-I particle) and was stored at -80°C until use.

To determine the size and purity of the isolated HL, samples were analyzed by SDS-PAGE on acrylamide gels, in the presence of  $\beta$ -mercaptoethanol and 6 M urea [15% running gel (pH8.8) and 4% stacking gel (pH 6.8)]. Duplicate gels were run and the proteins were either stained with 0.25% Coomassie R250 in acetic acid/methanol/H<sub>2</sub>O (2:9:9) and then destained in acetic acid/methanol/H<sub>2</sub>O (2:9:9) or they were electrophoretically transferred to polyvinylidene difluoride (PVDF) microporous membranes (Immobilon, Millipore, Bedford, MA). The HL was identified on the membrane by blotting initially with a mouse anti-human HL primary antibody, followed by a horse-radish peroxidase linked secondary antibody. Visualization was carried out using ECL™ Western blotting detection reagents (RPN2106, Amersham Life Sciences).

***Preparation of [<sup>14</sup>C]-diolein.*** To study the effect of NAG on the substrate specificity and catalytic regulation of HL, reconstituted Lp2A-I particles were prepared with [<sup>3</sup>H]-triolein and [<sup>14</sup>C]-diolein and then incubated with the purified enzyme. [<sup>14</sup>C]-diolein was isolated after a 4-h incubation at 37 °C of 5  $\mu$ Ci di[1-<sup>14</sup>C]oleoyl phosphatidylcholine, 1 ml of 0.2 units/ml phospholipase C in phosphate buffer (pH 7.3), 1 ml of 1% CaCl<sub>2</sub>, and 1 ml of diethyl ether. The reaction was stopped with five drops of 0.1 M HCl and then the DG was extracted with 5 ml of chloroform:methanol (1:1). After centrifugation for 15 min. at 2200 rpm, the lower phase was removed and dried under nitrogen. Preparative TLC, utilizing Silica Gel 60 plates and a solution of chloroform:acetone:methanol:acetic acid:water (60:80:20:20:10), was used to separate

the DG from unreacted substrate.

***Substrate incubations with hepatic lipase.*** Native and reconstituted Lp2A-I were characterized as substrates for purified HL using a standard assay system. Each enzyme assay contained the lipoprotein substrate, 214 units of purified HL, 3 mg of bovine serum albumin (essentially fatty acid free), 1.5 mM CaCl<sub>2</sub> and 1M NaCl in a 0.15 M Tris buffer (final vol = 500 μL). Incubations were carried out for 3 hours at 37°C and were terminated by placing the tubes in an ice bath. The total amount of fatty acids released during the incubation was determined using an enzyme kit assay from Boehringer Mannheim. The phospholipid, TG and DG hydrolytic rates were determined subtractively after measuring the quantity of radioactive fatty acids liberated from [<sup>3</sup>H]-triolein and [<sup>14</sup>C]-diolein during the incubation with HL using the liquid-liquid partitioning system of Belfrage and Vaughan (93). Under these conditions, <0.25% of the substrates and products (other than fatty acids) were recovered in the supernatant aqueous phase at both low and high substrate concentrations, while 72% of the fatty acids were retrieved (93). Subtraction of the TG- and DG-hydrolysis values from the total yielded the phospholipid hydrolytic rate. Initial rates were estimated with minimal substrate conversion.

## RESULTS

### *Section I: HDL structural analysis*

#### *Characterization of the size and composition of Lp2A-I and native HDL particles.*

Spherical reconstituted HDL particles (Lp2A-I) were prepared to contain POPC, apoA-I and various amounts of TG and DG (Table 3). Any lipids that did not associate with protein during the sonication process were removed by chromatographic reisolation of the particles. This resulted in a decrease in the ratios of lipids compared to apoA-I. POPC decreased from 60-68% of the initial composition, while the amounts of DG and TG decreased from 55-80% of the starting ratios (Table 3). Once reisolated, all the recombinant complexes exhibited only one band on nondenaturing gels (Figure 4). The hydrodynamic diameter of the particles was determined from nondenaturing gradient gel electrophoresis to  $\pm 0.5$  nm (SD) (Table 3). The size of these particles did not vary greatly from the average of 8.0 nm and can be considered similar to HDL<sub>3c</sub> in diameter (62).

In this study, normolipidemic HDL<sub>2</sub> protein content averaged 36% while HDL<sub>3</sub> had 55% protein by weight (Table 4). HDL<sub>2</sub> contained approximately 5% total NAG (TG, DG and MG) by weight while HDL<sub>3</sub> contained only about 2% NAG by weight. Total cholesterol (FC and CE) can vary greatly in normolipidemics, with an average of 35% by weight for HDL<sub>2</sub> and 12% for HDL<sub>3</sub>, while PL content ranged from 24 to 31% for HDL<sub>2</sub> and HDL<sub>3</sub>, respectively. Because the native HDL particles were so heterogeneous in nature, it was not possible to obtain one discernible band on non-denaturing gels, however, HDL<sub>2</sub> normally possesses an average size of 12 nm while HDL<sub>3</sub> would be around 8 nm (4). Electrophoretic

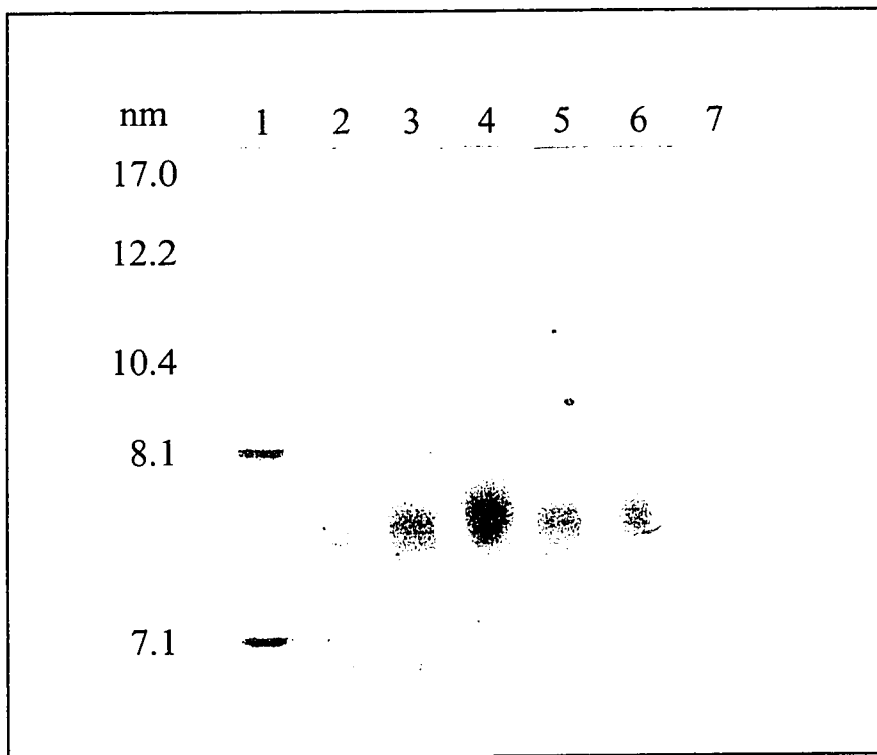


**Figure 4.** Reconstituted spherical Lp2A-I subjected to electrophoresis in 8-25% nondenaturing gels. Original gel profiles are shown for high molecular weight standards (lane1) and 6 different Lp2A-I particles with the following POPC:DG:TG:apoA-I compositions: 120:0:0:2 (lane 2), 120:0:40:2 (lane 3), 120:40:0:2 (lane 4), 120:10:20:2 (lane 5), 120:40:10:2 (lane 6), and 120:10:40:2 (lane 7). The molar ratios of each Lp2A-I were determined after chromatographic reisolation and are indicated in Table 3. Stokes' diameters were determined by comparison to high molecular weight standards. Lp2A-I particles exhibited a single discrete band, the size of which ranged between 7.5 and 8.0 nm.

**Table 3.** Composition and physical parameters of various Lp2A-I.

Particle composition <sup>a</sup> POPC:DG:TG:apoA-I (mol:mol:mol:mol)		NGGE size <sup>b</sup>
Initial	Final	nm
120-0-0-2	80-0-0-2	8.0
120-0-20-2	72-0-14-2	8.0
120-0-40-2	74-0-26-2	7.5
120-10-40-2	72-6-26-2	7.5
120-10-20-2	70-6-12-2	7.5
120-20-10-2	80-12-6-2	8.0
120-40-10-2	81-32-8-2	7.5
120-40-0-2	74-22-0-2	8.0
120-20-0-2	72-12-0-2	8.0

<sup>a</sup> LpA-I composition of phosphatidylcholine (POPC  $\pm$  10 mol), diacylglycerol (DG  $\pm$  3 mol), triacylglycerol (TG  $\pm$  3 mol) and apoA-I were determined after chromatographic reisolation as described in the text.

<sup>b</sup> Hydrodynamic diameter determined from non-denaturing gel electrophoresis using reference globular proteins ( $\pm$  0.5 nm SD)

**Table 4.** Molecular composition of native HDL particles

	Total Chol	Composition (% by weight)		Protein
		PL	NAG	
Hyperlipidemic				
HDL <sub>2</sub>	44	15	8	33
HDL <sub>3</sub>	28	26	6	40
Normolipidemic				
HDL <sub>2</sub>	35	24	5	36
HDL <sub>3</sub>	12	31	2	55

migration of both subspecies on an agarose gel led to a characteristic  $\alpha$ -migration (from -10.5 mV to -12.5 mV).

The native HDL isolated from hyperlipidemic patients had different compositions when compared to those from the normal subjects (Table 4). The protein levels varied from 33% by weight for HDL<sub>2</sub> to 40% for HDL<sub>3</sub>. Total cholesterol in the HDL<sub>2</sub> subspecies averaged around 44% by weight while it was closer to 28% in HDL<sub>3</sub>. There was an increase in total NAG over normal values for both HDL<sub>2</sub> (8%) and HDL<sub>3</sub> (6%). PL was found to be only 15% of the lipoprotein weight for HDL<sub>2</sub>, while it was 26% for HDL<sub>3</sub>. The Lp2A-I particles shown in Table 3 were synthesized to mirror the diversity of native HDL and to represent those isolated from both normolipidemics and hyperlipidemics.

*Effect of Lp2A-I core composition on the net charge of apoA-I.* To determine surface charge characteristics of HDL, the electrophoretic mobilities of these particles in 0.5% agarose gels were measured as described by Sparks and Phillips (17, 18). The net negative charge varied and was dependent on Lp2A-I composition (Figure 5). The Lp2A-I particle with no lipid core had the least negative charge with a surface potential of -9.1 mV. The inclusion of 20 molecules of TG resulted in an increased net negative charge, -9.4 mV, but this increase was not enhanced when the number of TG molecules was doubled (Figure 5). In the absence of TG, Lp2A-I particles with 20 molecules of DG also exhibited an increased negative charge of -9.7 mV yet the highest negative surface potential of -11.0 mV was observed with Lp2A-I containing 40 molecules of DG. When both TG and DG were present in the lipoprotein, the particle charge was proportional to the amount of DG present (Figure 5).

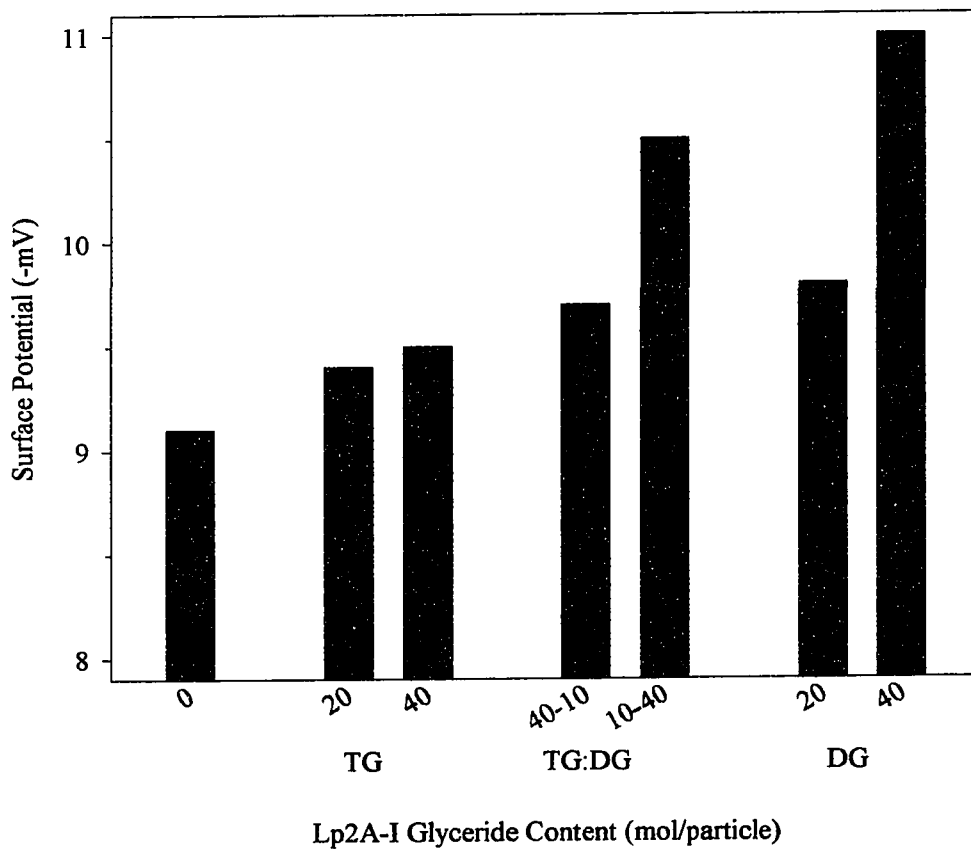


**Figure 5:** Effect of Lp2A-I glyceride composition on apoA-I net negative charge. Spherical Lp2A-I were prepared by co-sonication as described in the experimental procedures and particle surface charge was determined by electrokinetic analysis of their electrophoretic mobilities in 0.5% agarose gels.

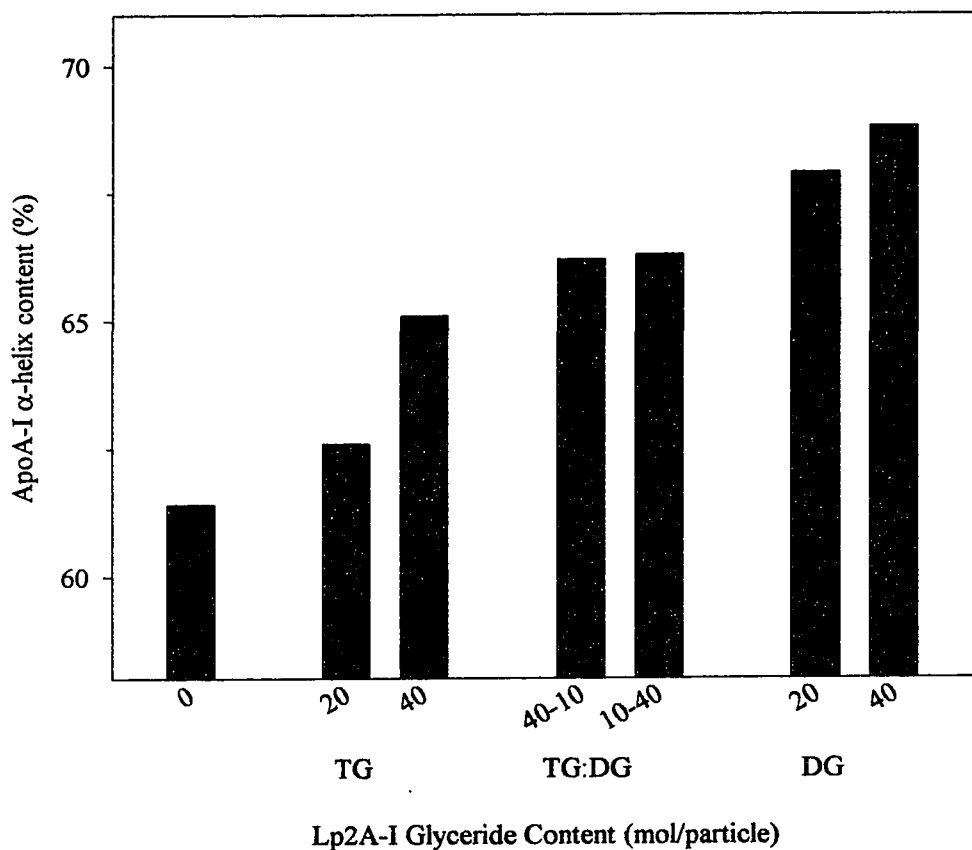


**Figure 6:** Effect of Lp2A-I glyceride composition on apoA-I  $\alpha$ -helix content. Spherical Lp2A-I were prepared by co-sonication and the content of  $\alpha$ -helices in apoA-I were determined by circular dichroism spectroscopy. The percent  $\alpha$ -helix in apoA-I on the different Lp2A-I particles was calculated from the molar ellipticities at 222nm using a mean residue weight of 115.3.

***Effect of Lp2A-I neutral glyceride composition on the secondary structure of apoA-I in Lp2A-I.*** The percent  $\alpha$ -helical content in apoA-I in different Lp2A-I particles was calculated by circular dichroism spectroscopy from the molar ellipticities at 222nm. In a spherical particle containing 2 molecules of apoA-I and 120 molecules of POPC, apoA-I exhibited an  $\alpha$ -helix content of 62% (Figure 6). Inclusion of 40 molecules of DG into the complex significantly increased the  $\alpha$ -helix content to 69%. In contrast, inclusion of similar amounts of TG into such a particle only slightly increased the content of  $\alpha$ -helix in apoA-I (65%). A smaller amount of TG (20 molecules) did not result in a significant change in  $\alpha$ -helicity. When both DG and TG were included into the lipoprotein, an intermediate  $\alpha$ -helix content (66%) was obtained (Figure 6).

***Isothermal denaturation of apoA-I in Lp2A-I.*** The effect of Lp2A-I glyceride content on the thermodynamic stability of apoA-I was measured by GdnHCl denaturation.  $\Delta G_D^\circ$  was calculated from the intercept on the vertical axis of linear regression plots of the observed free energies of denaturation ( $\Delta G_D$ ) against  $RT\ln(1+ka)$ . The absence of core lipids in an Lp2A-I sonicated particle gave rise to a rapid denaturation and a relatively unstable state, with a  $\Delta G_D^\circ$  value of 1.4 kcal/mol apoA-I (Figures 7 & 8). Inclusion of 20 molecules of DG and 10 molecules of TG protected apoA-I from denaturation and appeared to increase apoA-I stability in GdnHCl (Figure 7A). Increasing the DG content to 40 molecules also protected the  $\alpha$ -helices of apoA-I from denaturing and led to an increase in the overall stability to 2.2 kcal/mol. Inverting the DG/TG ratios so that 40 molecules of TG and 10 molecules of DG were incorporated into Lp2A-I, resulted in a reduced thermal stability to 1.6 kcal/mol (Figure 8). This value was found to be similar to Lp2A-I containing TG but

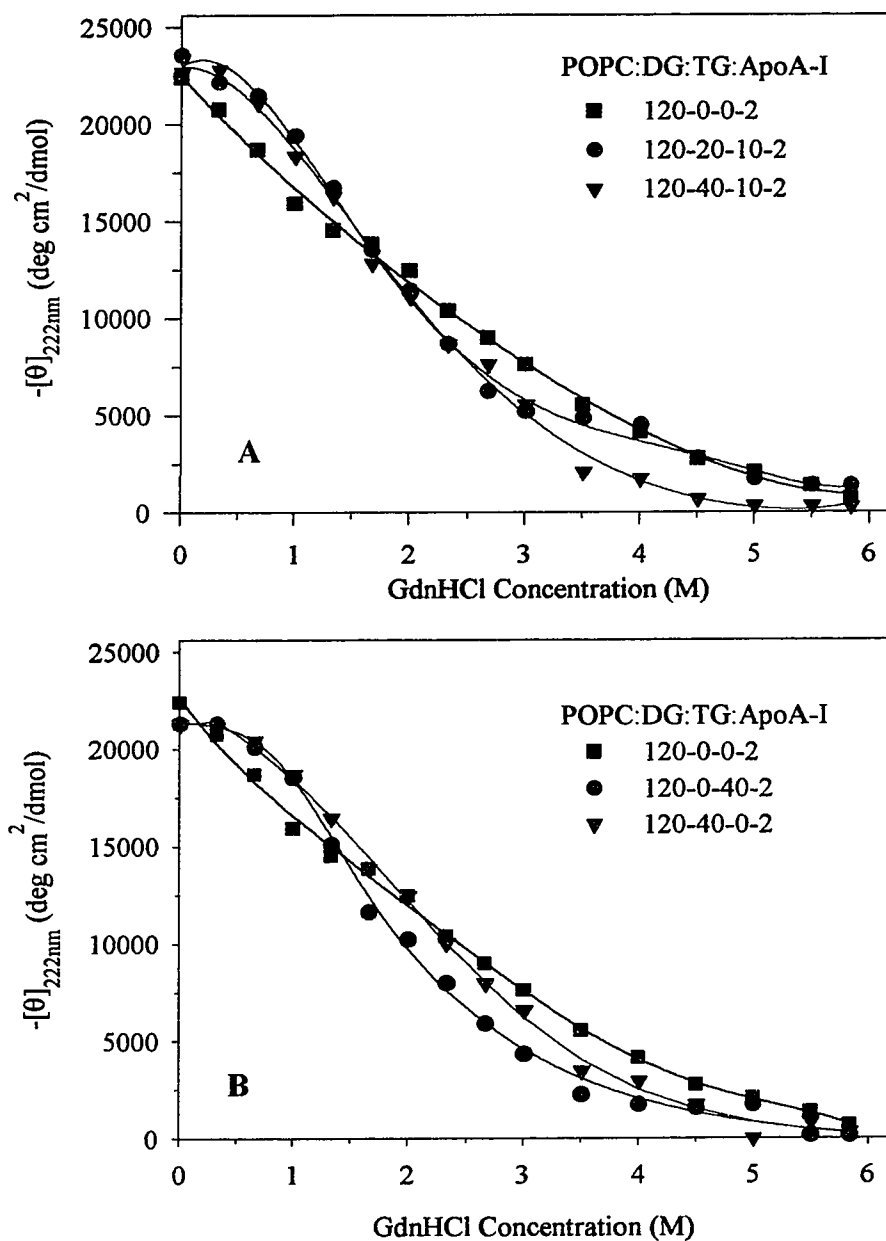


**Figure 7:** Effect of Lp2A-I glyceride content on the molar ellipticity of apoA-I during GdnHCL denaturation. Aliquots of spherical Lp2A-I (POPC:DG:TG molar ratios, panel A: ■, 120-0-0-2; ●, 120-20-10-2; ▼, 120-40-10-2; panel B: ■, 120-0-0-2; ●, 120-0-40-2; ▼, 120-40-0-2) were incubated with 0-6 M GdnHCl in 0.05 M phosphate buffer for 72h at 4°C. CD values were measured at 222nm at 24°C in a 0.1 cm pathlength quartz cell with sample protein concentrations of 33.3 μg/mL phosphate buffer.

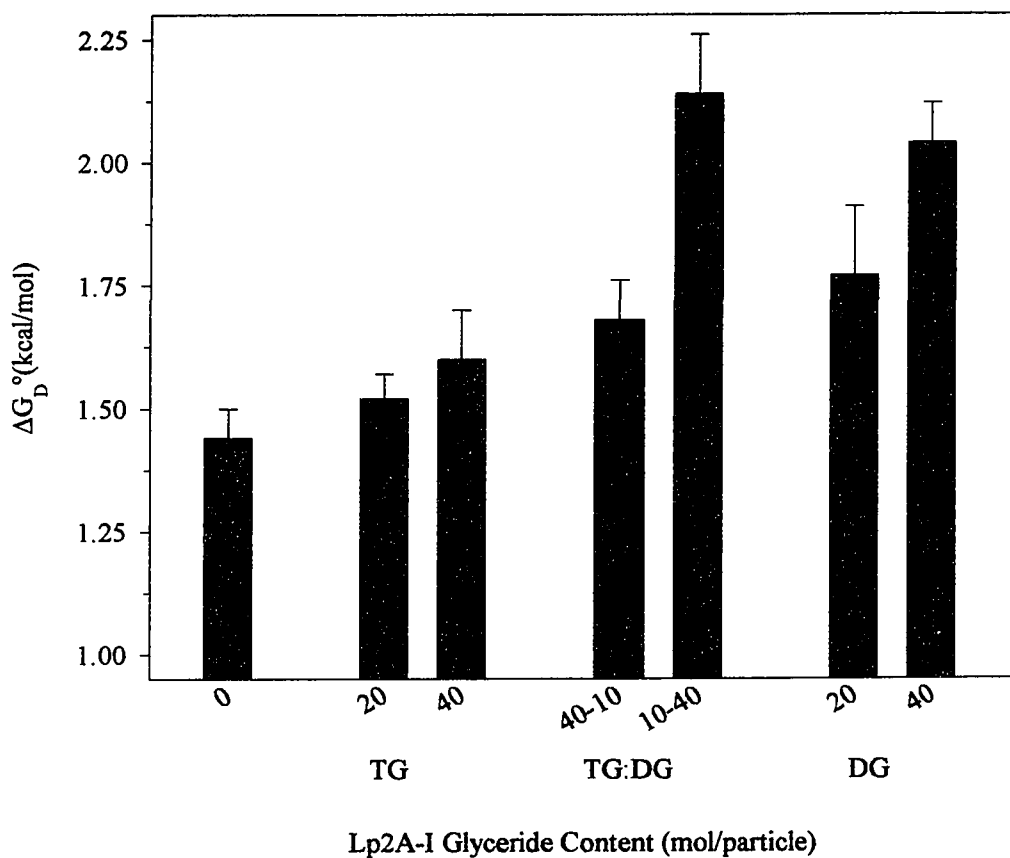


**Figure 8:** Effect of Lp2A-I glyceride composition on apoA-I thermal stability. The free energies of denaturation at zero GdnHCl concentration ( $\Delta G_D^\circ$ ) for various Lp2A-I particles (Table 3) were calculated from the intercept on the vertical axis of linear regression plots of the observed free energies of denaturation ( $\Delta G_D$ ) against  $RT\ln(1+ka)$ .

devoid of DG. In contrast, inclusion of 40 molecules of DG, in the absence of TG, resulted in a  $\Delta G_p^\circ$  value of 2.1 kcal/mol. The denaturation of  $\alpha$ -helices in apoA-I by GdnHCL may be inhibited, therefore, in the particles containing DG as compared to those containing a similar amount of TG (Figures 7B and 8).

*Effect of neutral glyceride content on the immunoreactivity of apoA-I.* A competitive radioimmunoassay (RIA) was used to detect differences in apoA-I conformation on the different Lp2A-I complexes. The eight mAbs used interact with defined epitopes over most of the apoA-I sequence (Figure 9). Two representative competition curves are shown in Figure 10.  $B/B_0$  represents radioactivity bound in the presence/absence of competitor. The monoclonal antibody 4H1 corresponds to an epitope at the extreme amino-terminus of apoA-I, at residues 2 to 8 (61). This region was most exposed in the absence of either TG or DG, as represented by the curve for the 120-0-0-2 particle which is furthest to the left on the  $B/B_0$  versus antigen concentration graph (Figure 10A). The antigen concentration at which half maximum binding of the antibody is attained is called the  $ED_{50}$ . These values were calculated from the linear region of the curves shown in Figure 10 and are shown in Figures 11 and 12 for a variety of antibodies and Lp2A-I. The  $ED_{50}$  value of  $4.1 \pm 0.3 \mu\text{g/ml}$  represents the concentration of 120-0-0-2 particle at which half of the maximum binding of the antibody 4H1 was attained (Figure 11A). Inclusion of TG decreased this exposure by 4 fold, shown by a shift to the far right of the curves in Figure 10A and an increase in  $ED_{50}$  in Figure 11A. DG decreased the immunoreactivity approximately 2 fold (Figures 10A and 11A), as shown by intermediate shifts in the binding curves and corresponding  $ED_{50}$  values.

The mAb 2G11 recognizes a number of different domains within a broad region

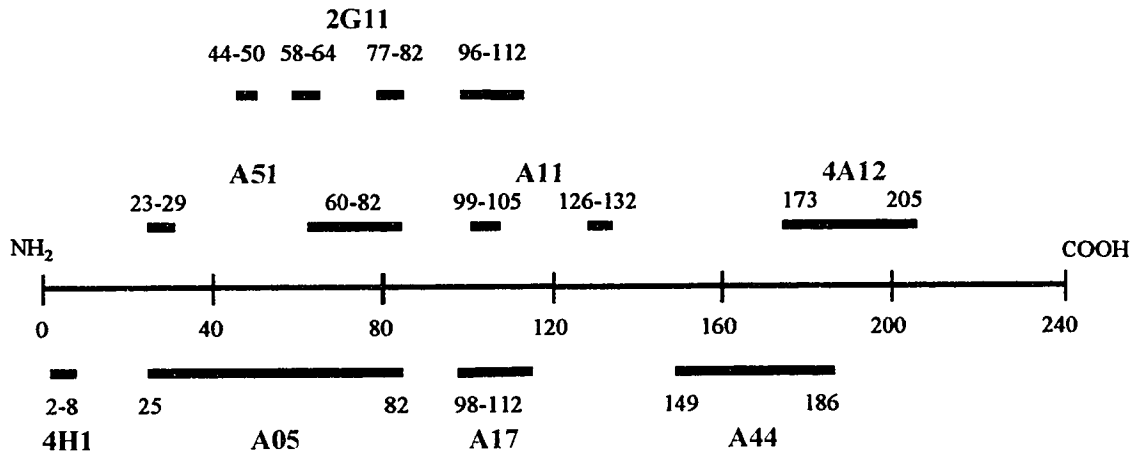


**Figure 9:** A linear epitope map of apolipoprotein A-I. Each epitope is identified by the name of the mAb, in blue, and a sequence bar delineating the epitope boundaries, in red. Antibodies with discontinuous epitopes are represented by more than one red sequence bar. Adapted from Marcel *et al.* (61).

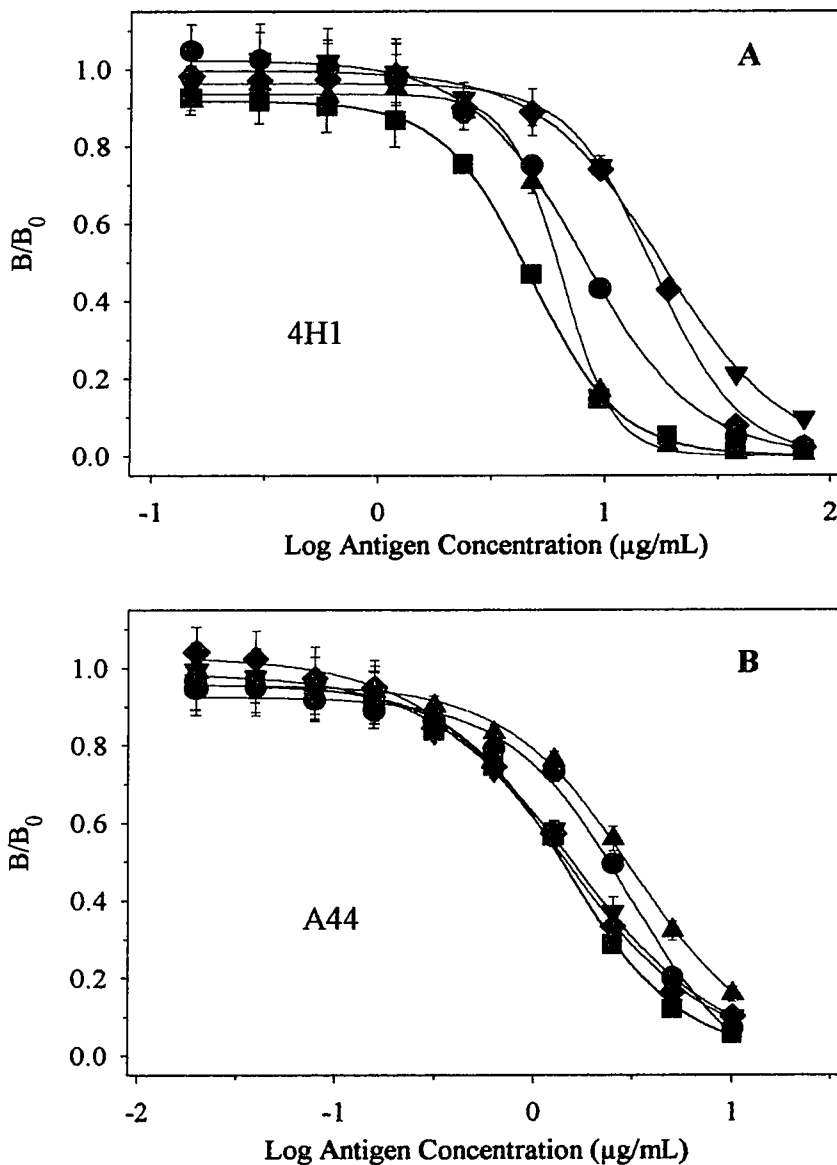


**Figure 10:** Effect of Lp2A-I glyceride content on ApoA-I immunoreactivity as measured by competitive radioimmunoassay (RIA). A panel of anti-apoA-I mAbs were appropriately diluted and incubated with dilutions of Lp2A-I (POPC:DG:TG:apoA-I molar ratios: ■, 120-0-0-2; ◆, 120-0-40-2; ▼, 120-10-40-2; ●, 120-40-10-2; ▲, 120-40-0-2) on apoHDL-coated microtitre wells, as indicated in the experimental procedures. Bound anti-apoA-I mAbs were detected with  $^{125}\text{I}$ -anti-mouse IgG. Competition curves for 2 representative mAbs are shown (panel A, 4H1 and panel B, A44).  $B/B_0$  represents radioactivity bound in the presence of competitor as a fraction of that bound in the absence of competitor.

between the amino-terminus and the central domain of apoA-I. This antibody covers four epitopes: 44-50, 58-64, 77-83 and 96-112, including potentially discontinuous areas within the tertiary structure of the protein (61). Marcel *et al.* (61) proposed that the folding of the peptide chain could bring together sequences that would otherwise be far apart and thus form complex tertiary discontinuous epitopes. Of the antibodies investigated in this study, 2G11 contained the most diverse group of domains and seemed to be affected by the inclusion of 10 molecules of DG and 40 molecules of TG (Figures 9 and 11B). The ED<sub>50</sub> value for this particle was 45 ± 4 µg/ml; 3.5 fold larger than the Lp2A-I containing no NAG. The other particles did not vary significantly from the control.

Two antibodies, A05 and A51, recognized epitopes within the same domain of an amino-terminal region of apoA-I. A05 recognized an epitope from amino acids 25 to 82 while A51 recognized two domains, from 23 to 29 and 60 to 82. These epitope differences are associated with slightly different affinities between the particles and the two antibodies. The ED<sub>50</sub> for the 120-0-0-2 particle with A05 was 2.4 ± 0.2 µg/ml while with A51 it was 1.7 ± 0.1 µg/ml (Figure 11C & D). Inclusion of any amount of glyceride decreased the immunoreactivity of A05 with its epitope (from 1.5 to 2 fold). Inclusion of 40 molecules of TG, in the absence of DG, slightly decreased the immunoreactivity of A51. Inclusion of both glycerides increased the immunoreactivity by 2.5 to 3 fold, while DG alone caused a lesser increase.

The calculated ED<sub>50</sub> values for the mAbs that recognized epitopes in the central to carboxy terminus of apoA-I are shown in Figure 12. A17 recognized a domain at residues 98-112 and showed an ED<sub>50</sub> of 0.71 ± 0.03 µg/ml for the control particle. Inclusion of DG did not alter the immunoreactivity significantly, however, TG decreased this interaction by

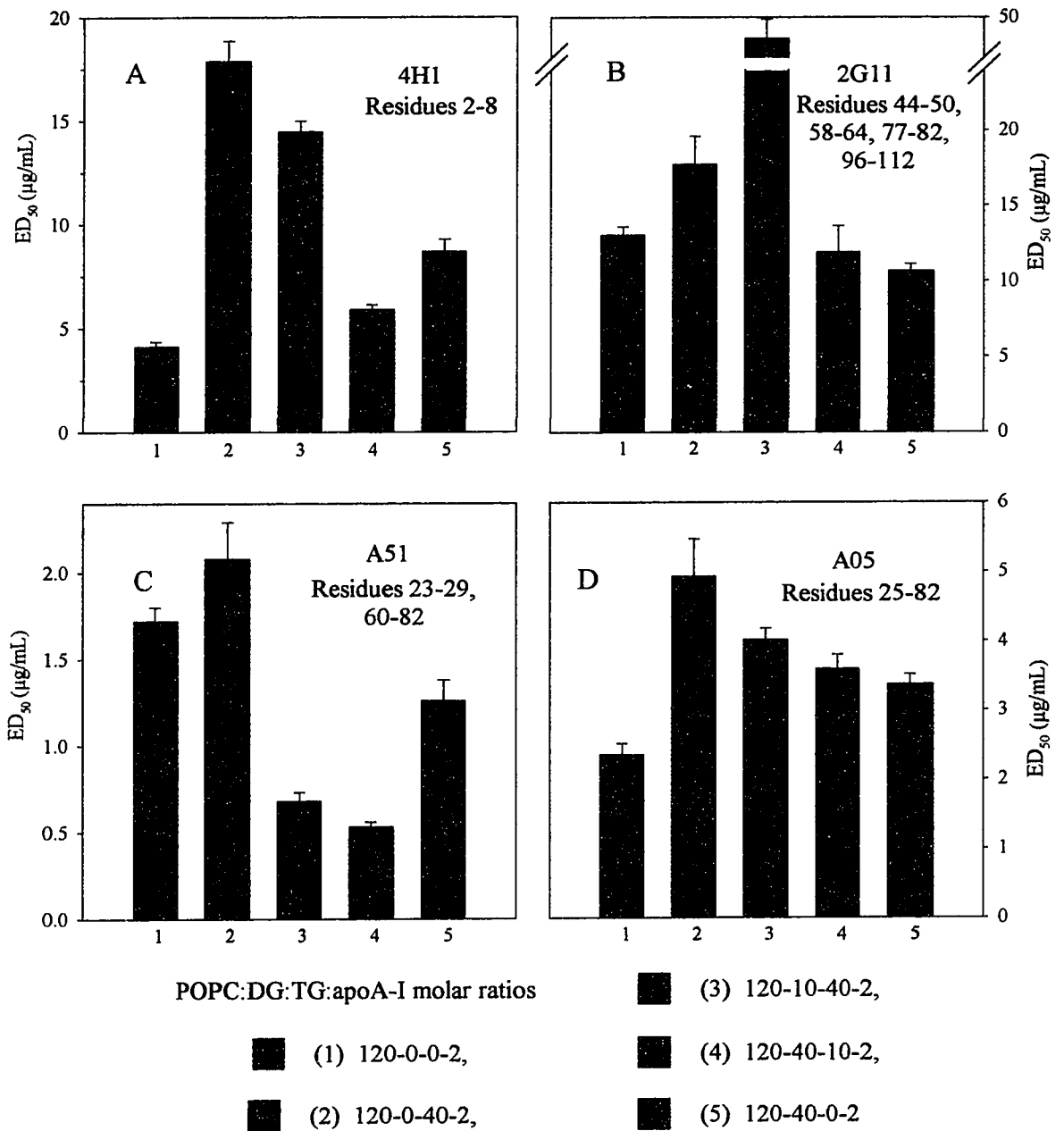


**Figure 11:** Effect of Lp2A-I glyceride content on the exposure of epitopes in the N-terminal domain of apoA-I. As indicated in the text, ED<sub>50</sub> values were calculated from the linear region of the curves shown in Figure 10 for a variety of antibodies and Lp2A-I. The ED<sub>50</sub> values represent the antigen concentration at which half maximum binding of the antibody is attained.

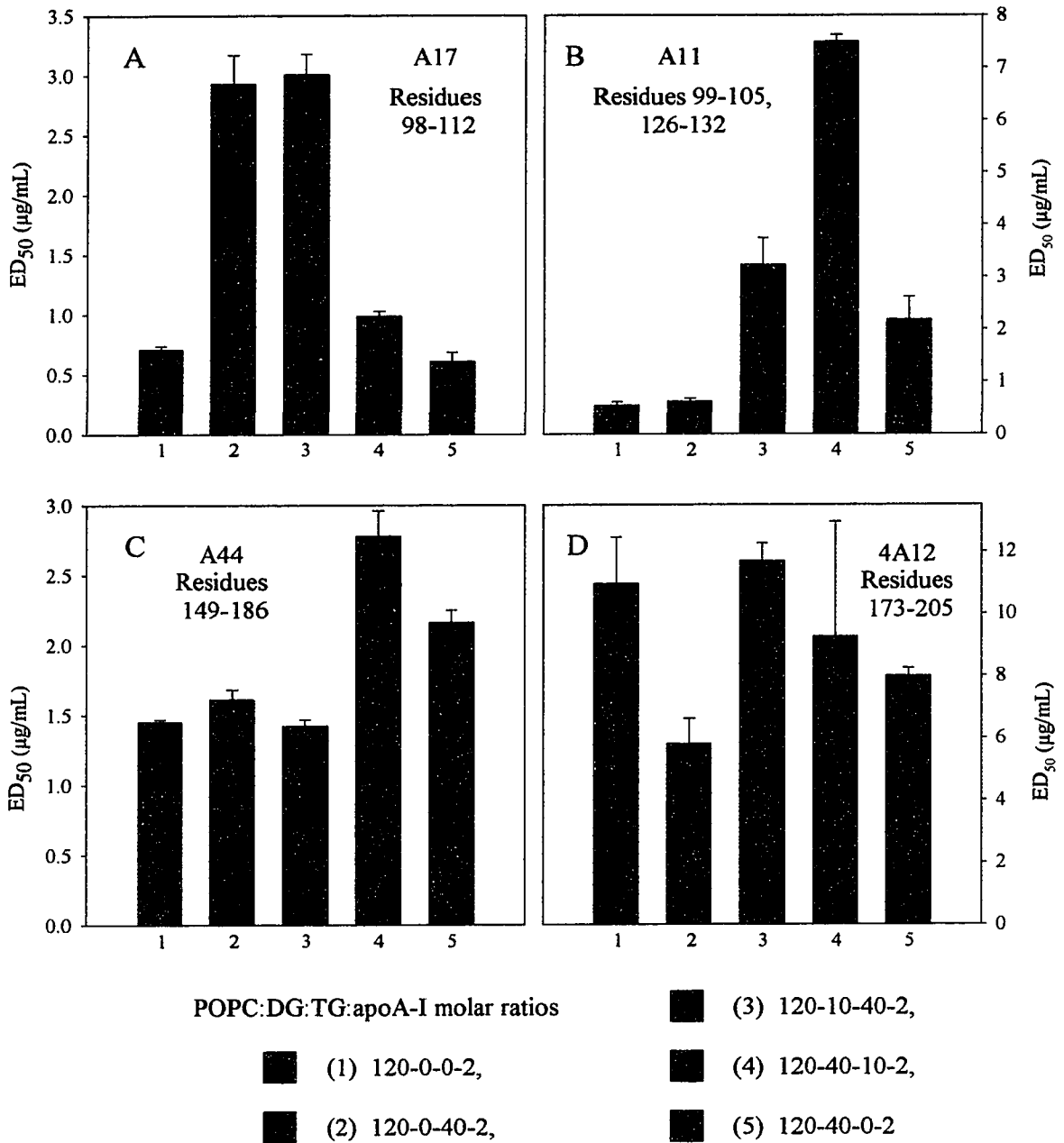


**Figure 12:** Effect of Lp2A-I glyceride content on the exposure of epitopes in the C-terminal domain of apoA-I. As indicated in the text, ED<sub>50</sub> values were calculated from the linear region of the curves shown in Figure 10 for a variety of antibodies and Lp2A-I. The ED<sub>50</sub> values represent the antigen concentration at which half maximum binding of the antibody is attained.

3 fold (Figure 12A). The antibody A11 shared an epitope with A17 between amino acids 99-105 and, in addition, reacted with residues 126 to 132. Not surprisingly, these two mAbs showed a similar  $ED_{50}$ ,  $0.54 \pm 0.07 \mu\text{g/ml}$ , with the control particle (Figure 12B). Inclusion of TG alone did not have an effect on mAb affinity, yet the presence of 10 molecules of TG and 40 of DG greatly decreased the immunoreactivity of this epitope by 14 fold. Inclusion of DG alone or 40 molecules of TG with 10 molecules of DG also decreased the reactivity by 4 and 6 fold, respectively.

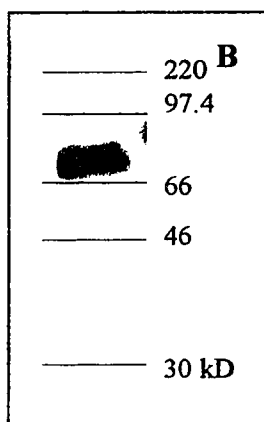
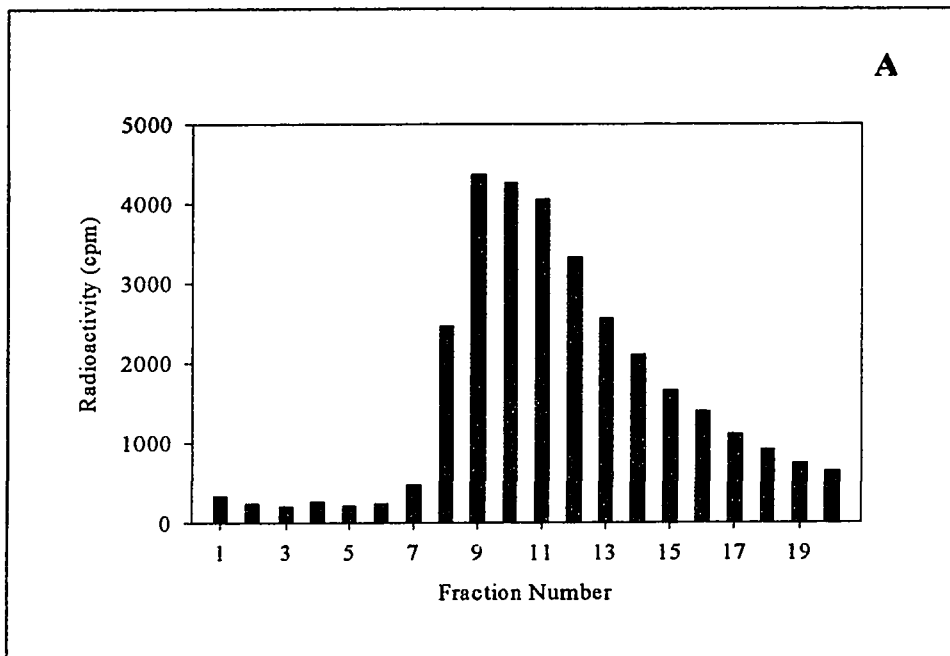
The monoclonal antibody A44 recognized an epitope between the centre and the carboxyl-terminus of apoA-I, amino acids 149 to 186. The presence of TG or the absence of both glycerides resulted in similar curves in Figure 10B and thus similar  $ED_{50}$  values of  $1.5 \pm 0.1 \mu\text{g/ml}$  (Figure 12C). Inclusion of DG into the Lp2A-I particles, however, shifted the curves to the right (Figure 10B) and decreased the epitope exposure (Figure 12C).

The mAb with the most carboxyl terminal epitope, amino acids 173 to 205, is 4A12. The particle with 120-0-0-2 composition showed an  $ED_{50}$  of  $11 \pm 1 \mu\text{g/ml}$ . There was no significant change in this value with the addition of both DG and TG into the Lp2A-I particle but the inclusion of TG alone increased the immunoreactivity of the epitope by 2 fold. Inclusion of 40 molecules of DG, in the presence or absence of TG, slightly increased the binding of the antibody.

## ***Section II: HDL and hepatic lipase***

***Purification of human hepatic lipase.*** HL was purified from postheparin plasma drawn from normolipidemic subjects by a two step protocol involving lipid emulsion extraction and then heparin sepharose affinity chromatography. A 20% TG emulsion was incubated with the plasma to bind the more lipophilic proteins and to allow their isolation by centrifugation. To separate HL from lipoprotein lipase (LPL) and from other proteins that may have been recovered with the fat cake, heparin sepharose affinity chromatography was utilized. HL has a lower affinity than LPL for heparin so a lower ionic strength wash was applied to elute HL, but not LPL, from the heparin sepharose column. The elution profile from this column during the 0.9M NaCl step gave a single protein peak based on absorbance at 260 nm (data not shown) and a well-defined hydrolytic activity (Figure 13A). Only those fractions with a hydrolytic activity above 3500 cpm of [<sup>3</sup>H]oleic acid release per hour were collected for further use. To confirm the presence of HL in the column eluent, 15% PAGE was performed followed by western blotting (Figure 13B). A single band corresponding to human HL was visible at an approximate size of 69 kD and within the expected range for this glycoprotein (40, 86, 88). The specific activity of the HL was greatly enhanced after the heparin-sepharose isolation as the hydrolytic activity of the eluent was high for the amount of protein collected. This resulted in a 600-fold purification. The purified HL was tested periodically during storage over 1 year and it showed no losses in activity (data not shown).

***Lipid hydrolysis in native HDL by hepatic lipase.*** Native HDL isolated by



**C**

Sample	Specific Activity $\mu\text{eq}/\text{mg}/\text{h}$	Purification Factor - fold
Plasma	1.1	--
Heparin-Sepharose	675	600

**Figure 13:** Purification of human hepatic lipase. Post-heparin plasma was obtained from normolipidemic subjects and a preparation of crude hepatic lipase was achieved as described in the text. Panel A shows the hydrolytic activity of the fractions obtained from the heparin-sepharose column during the 0.9M NaCl elution (■ denotes the pooled fractions of purified hepatic lipase used in further experimentation). Panel B is a western blot with a mouse polyclonal antibody (1:10,000 dilution) against the isolated human hepatic lipase (1.5  $\mu\text{g}$ ) after 15% SDS-PAGE. The horizontal lines denote protein markers of the sizes depicted. Panel C shows the change in specific activity and fold purification between the post-heparin human plasma and the isolated hepatic lipase.

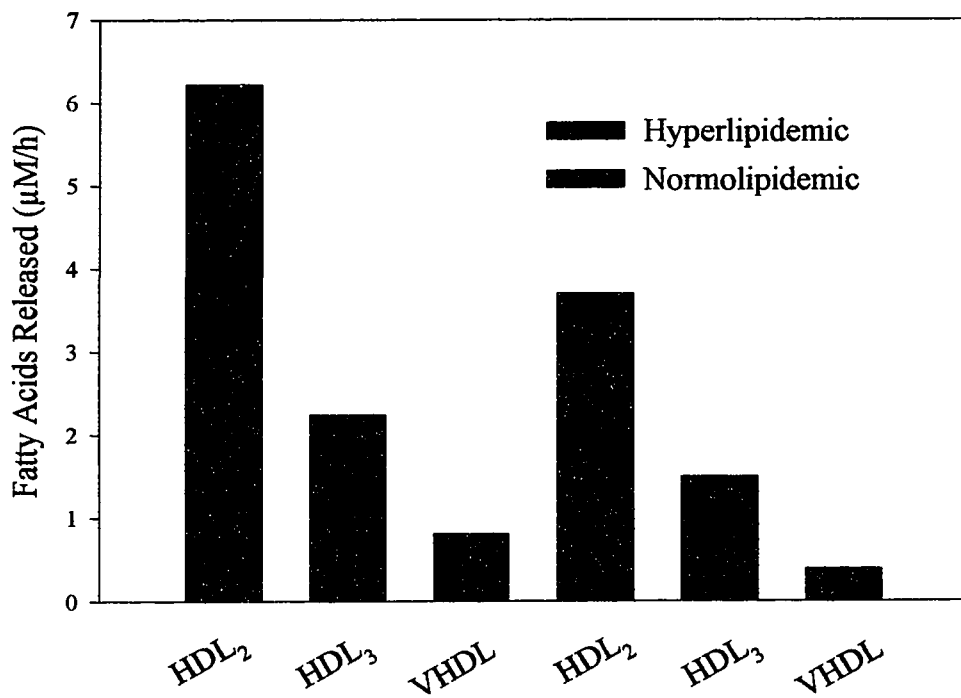


**Figure 14:** Hepatic lipase total hydrolytic activities with native lipoproteins isolated from hyper- and normolipidemic subjects. HDL subfractions were obtained by ultracentrifugation as described in the text and then incubated with purified HL for 3h. Equal phospholipid concentrations (200 µM) were used for each substrate.

sequential ultracentrifugation, from both hyper- and normolipidemic subjects, were incubated with purified HL. The liberated free fatty acids were then measured using a commercially available enzyme kit (Boehringer Mannheim). The relative total rates of lipid hydrolysis for the different HDL subfractions were similar to that described by others (95, 96). As substrates for HL, the HDL isolated from the hyperlipidemic patients were better than those from the normolipidemic subjects (Figure 14). The hyperlipidemic HDL<sub>2</sub> (h-HDL<sub>2</sub>) was the best substrate with a rate of 6.2 μM free fatty acids released per hour. Fatty acid release from normolipidemic HDL<sub>2</sub> (n-HDL<sub>2</sub>) was 40% decreased in comparison. The hydrolytic rates for normolipidemic HDL<sub>3</sub> and VHDL were 1/3 and 1/2 less than that observed for hyperlipidemic lipoproteins. In addition, there was a difference in the specificity of HL for the different HDL species. In both subjects, the hydrolysis of HDL<sub>2</sub> > HDL<sub>3</sub> > VHDL.

Native HDL<sub>2</sub> from both hyper- and normolipidemic subjects was incubated with [<sup>3</sup>H]-TG/POPC vesicles to incorporate radioactive TG into the lipoproteins. Labeled HDL<sub>2</sub> was incubated with HL to characterize both PL and TG hydrolytic rates. The hydrolysis of HDL lipids by HL was dependent on the concentration of substrate (Figure 15). Total hydrolysis measured by the FFA enzyme kit showed that over a 400 μM phospholipid concentration range the HDL<sub>2</sub> isolated from a hyperlipidemic patient consistently had higher activities than that from a normolipidemic subject (Figure 15A). At the highest substrate concentrations, the h-HDL hydrolysis was double that of the n-HDL (11.2 compared to 5.9 μM FFA/h). In addition, the TG hydrolysis by HL was substantially higher for the hyperlipidemic subject over the same concentration range (Figure 15B). The n-HDL had a hydrolytic rate of 0.26 μM FFA/h at the highest

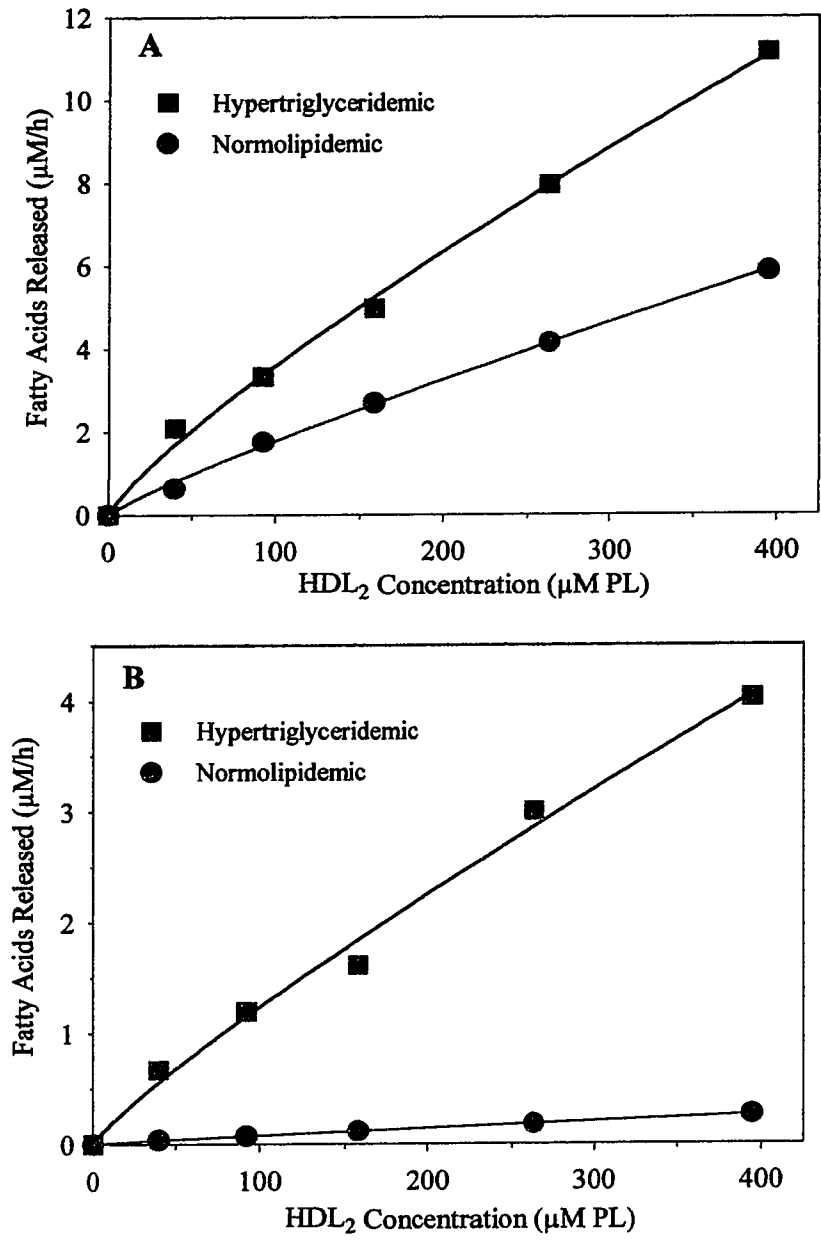


**Figure 15:** Hepatic lipase total and triacylglycerol hydrolytic activities with HDL<sub>2</sub> isolated from hypertriglyceridemic and normolipidemic subjects. HDL<sub>2</sub> was labeled with [<sup>3</sup>H]triolein as described in the text and then incubated with purified HL for 3h. HL mediated hydrolysis of total lipids (Panel A) and triacylglycerol (Panel B) in HDL<sub>2</sub>. Increasing amounts of substrate were used based on phospholipid concentrations. Hydrolytic values are the mean of duplicate determinations.

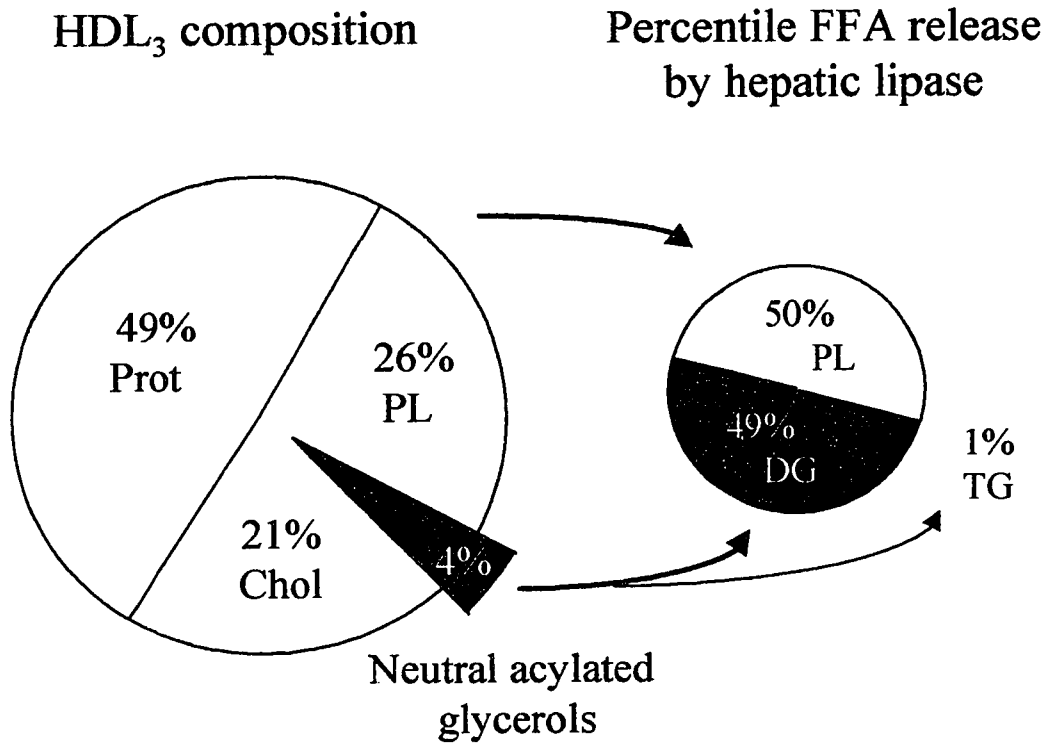


**Figure 16:** The hydrolysis of polar and nonpolar lipids in HDL<sub>3</sub> by HL. Normolipidemic HDL<sub>3</sub> was labeled with [<sup>3</sup>H]triolein and [<sup>14</sup>C]diolein as described in the text and then incubated with purified HL for 3h. HDL<sub>3</sub> protein (Prot), total cholesterol (Chol), phospholipid (PL) and neutral acylated glycerol composition (% by weight) is shown (left pie) relative to the percentage of fatty acids released from TG, DG and PL by HL (right pie).

concentration of substrate while the h-HDL rate was 15-fold higher.

To determine the specific rates of both DG and TG hydrolysis, a fasting normolipidemic HDL<sub>3</sub> sample was incubated with [<sup>3</sup>H]-TG+[<sup>14</sup>C]-DG/POPC vesicles. After an 8 h incubation >90% of the tracers were incorporated. The amount of DG and TG in the HDL<sub>3</sub> subfraction was quantified by preparative TLC and shown to be approximately 2.2:1, DG: TG. Determinations of HL-catalyzed lipid hydrolytic rates for the HDL<sub>3</sub> sample showed that only 1% of the fatty acids liberated were from TG, the balance came from DG and PL hydrolysis (Figure 16). Even though DG constituted only about 1% of the lipid weight of the HDL<sub>3</sub> particle, DG hydrolytic rates represent 49% of the total lipid hydrolysis. Hydrolytic rates for a fasting HDL<sub>2</sub> sample gave similar results, with 5% of fatty acids coming from TG and 30% coming from DG (data not shown).

*Effect of HDL surface lipids on lipid hydrolysis by hepatic lipase.* HDL<sub>3</sub> was isolated from a normolipidemic subject by sequential ultracentrifugation and then incubated with Celite (diatomaceous earth) containing 4 mg of unesterified cholesterol (FC), sphingomyelin (SPM) or phosphatidylinositol (PI) to alter the surface lipid composition. To characterize the effect that these surface lipids have on total lipid hydrolysis, the different HDL<sub>3</sub> were incubated with HL. The control HDL<sub>3</sub>, incubated with only Celite, showed increased total lipid hydrolysis with increased protein concentration (Figure 17A). At the highest substrate concentration used, the rate of fatty acids released was 16 μM/h. Incorporation of sphingomyelin caused a significant reduction (37%) in the total hydrolytic rate of HL when compared to the control. Phosphatidylinositol enrichment, however, resulted in a small increase (14%) in the total

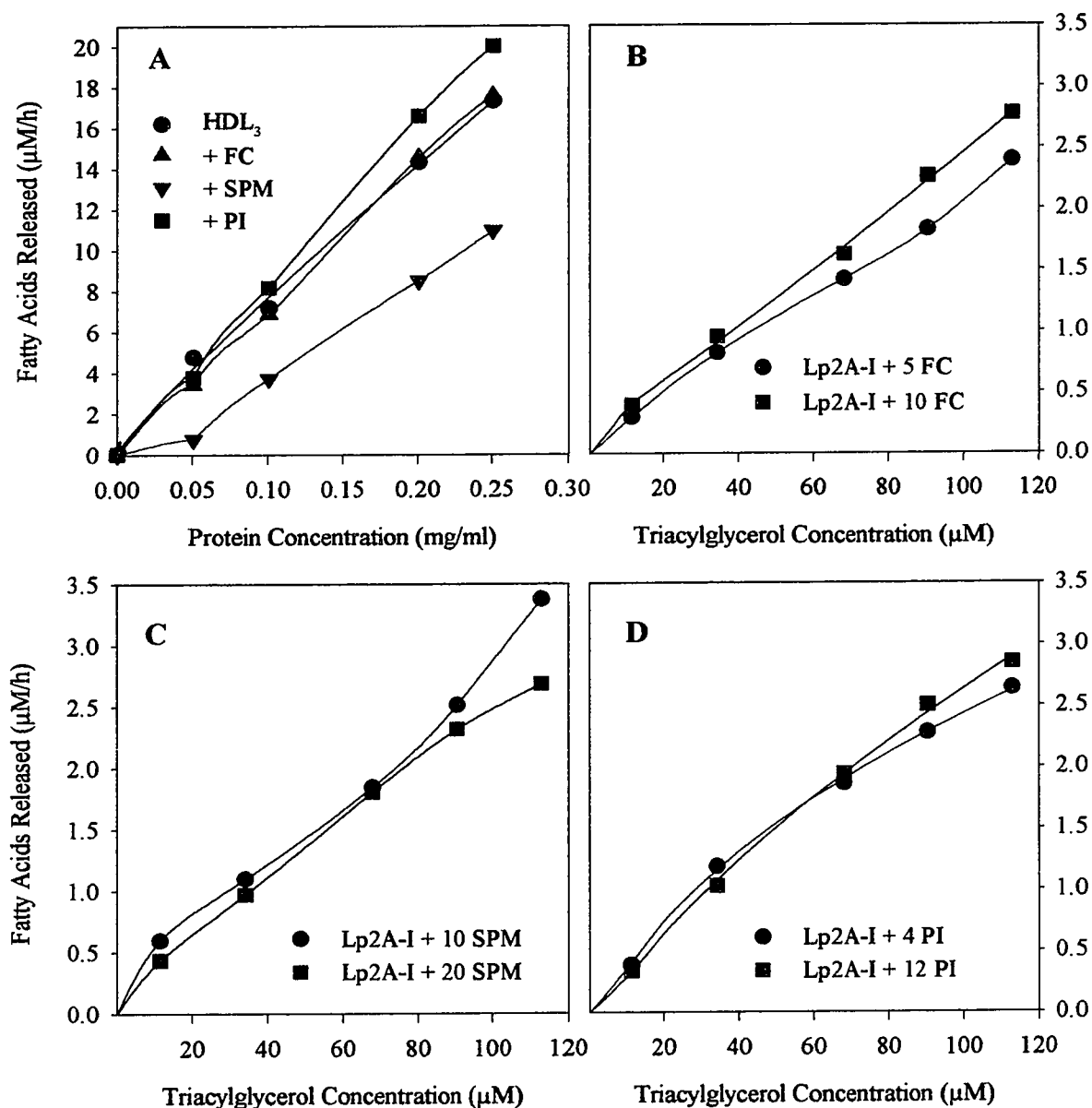


**Figure 17:** The effect of surface lipids on hepatic lipase total and triacylglycerol hydrolytic activities. Panel A: HL mediated hydrolysis of total lipids is shown. Normolipidemic HDL<sub>3</sub> was incubated with Celite and unesterified cholesterol (FC), sphingomyelin (SPM) or phosphatidylinositol (PI) as described in the text and then incubated with purified HL for 3h. Panels B, C and D: HL mediated hydrolysis of triacylglycerol is shown. Lp2A-I (120:20:2; POPC:TG:apoA-I molar ratios + moles of lipids shown) were prepared by co-sonication and were incubated with purified HL as described in the text.

rate. Incorporation of free cholesterol had little effect on the total hydrolysis of HDL<sub>3</sub> with HL.

As the hydrolysis of TG by HL may be affected by the altered HDL lipid composition in hyperTG patients (34, 86), various amounts of sphingomyelin, phosphatidylinositol and unesterified cholesterol (shown in Figure 17B-D) were incorporated into reconstituted HDL particles with a composition 120:20:2 (POPC:TG:apoA-I molar ratios). These particles also contained [<sup>3</sup>H]triolein so that the release of [<sup>3</sup>H]oleic acid could be monitored as an indication of HL TG lipolytic activity. In contrast to observations from other laboratories (56), adjusting the free cholesterol content did not greatly alter the lipid hydrolysis by HL (Figure 17B). All particles exhibited increased hydrolytic activities with increased TG concentration, however, at the highest TG concentration (117 μM), none of the particles varied more than 15% from the rate of 3.0 μM of free fatty acids released/h (Figure 17C & D). The hydrolysis of DG was not measured due to time constraints.

*Effect of Lp2A-I triacylglycerol content on hepatic lipase activity.* Figure 18 illustrates the rates of fatty acid liberation from both PC and TG in Lp2A-I containing various amounts of TG (see Table 5 for Lp2A-I compositions before and after particle reisolation). Incubation of HL and an Lp2A-I containing 120:2, PC:apoA-I (mol:mol) shows that these lipoproteins were good substrates for HL and that PC hydrolysis was the most rapid in Lp2A-I devoid of TG. Inclusion of 10 molecules of TG significantly reduced the phospholipase activity of HL and was associated with a small amount of TG hydrolysis. Inclusion of 20 molecules of TG also reduced the phospholipase activity of HL, but to a lesser extent than with particles containing only 10 molecules of TG. Similarly, inclusion of

**Table 5.** Effect of Lp2A-I lipid composition on the diacylglycerol, triacylglycerol and phospholipid hydrolytic activities of human hepatic lipase.

Particle composition <sup>a</sup> POPC:DG:TG:apoA-I (mol:mol:mol:mol)		Total Hydrolytic Rate <sup>b</sup>	Diacylglycerol Hydrolysis	Triacylglycerol Hydrolysis	Phospholipid Hydrolysis
Initial	Final				
<i>percentage of total hydrolysis (%)</i>					
120:0:0:2	82:0:0:2	7	--	--	100
120:0:10:2	70:0:8:2	3	--	26	74
120:0:20:2	72:0:14:2	7	--	26	74
120:0:40:2	74:0:26:2	42	--	43	57
120:10:40:2	72:6:26:2	40	61	17	22
120:10:20:2	70:6:12:2	38	55	9	36
120:20:10:2	80:12:6:2	63	49	3	48
120:40:10:2	81:32:8:2	143	96	3	1
120:40:0:2	74:22:0:2	89	97	--	3

<sup>a</sup> LpA-I composition of phosphatidylcholine (POPC,  $\pm 10$  mol), diacylglycerol (DG,  $\pm 3$  mol), triacylglycerol (TG,  $\pm 3$  mol) and apoA-I were determined after chromatographic reisolation as described in the text.

<sup>b</sup> Initial hydrolytic rates were determined from pseudo first-order kinetic analysis of the curves shown in Figures 18 and 19. Values, given as nM FA/h per  $\mu$ M PL, are representative of 3 different preparations of Lp2A-I.

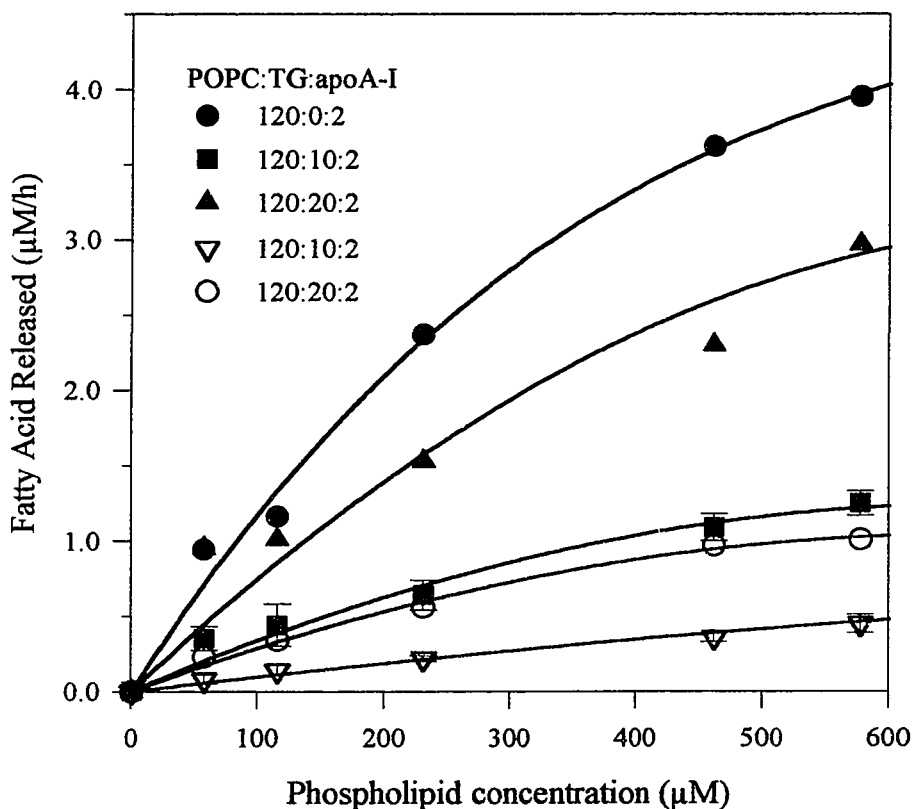


**Figure 18:** Effect of the triacylglycerol content of spherical Lp2A-I on HL activation. HL mediated hydrolysis of TG (open symbols) and POPC (solid symbols) in Lp2A-I particles containing various amounts of TG is shown. Lp2A-I were prepared by co-sonication (stoichiometries after reisolation are shown in Table 5) and were incubated with HL as described in the text. Hydrolytic values are  $\pm$  SD of triplicate determinations and are representative of 3 different preparations of Lp2A-I (SD error bars were generally smaller than the size of symbols and are therefore not shown for all curves).

twice as much TG into the Lp2A-I was associated with an almost 2-fold increase in TG hydrolysis. The estimated rates of hydrolysis and the relative contribution of TG, DG and PC hydrolytic rates for the data in Figures 18 and 19 is presented in Table 5. Although enzyme saturation conditions existed in the absence of DG (Figure 18), Lp2A-I containing DG were highly reactive with HL and gave rise to hydrolysis curves that were almost linear over the substrate concentration studied (Figure 19). The hydrolytic rates described in Table 5 were therefore expressed as pseudo first-order rate constants.

While incorporation of 10 or 20 molecules of TG into the Lp2A-I particles had different effects on the absolute rates of PC and TG hydrolysis, it was striking that with the different lipoprotein particles, exactly the same relative rates of lipid hydrolysis were evident, 74% PC and 26% TG hydrolysis (Table 5). Raising the TG content to 40 molecules, in the absence of DG, stimulated the overall lipid hydrolytic rates and modified the relative lipid hydrolytic rates (Table 5). The Lp2A-I particle with the composition of 120:40:2, POPC:TG:apoA-I (mol:mol) had the highest TG hydrolytic rate of the particles characterized. TG hydrolytic rate for this particle was 16.7 nM FFA/h/ $\mu$ M POPC and represented 43% of the total hydrolysis. Doubling the TG content of the Lp2A-I from 20 to 40 molecules, in the absence of DG, was therefore associated with a 6-fold increase in the total lipid hydrolytic rate and a shift in the contribution of each lipid substrate. The absolute hydrolysis of both PL and TG increased but there was a 17% reduction in the PC relative contribution with a parallel increase in TG percentage. Interestingly, once the NAG content of Lp2A-I was at 30 molecules or above, doubling the TG content from 20 molecules to 40 did not alter the total HL hydrolytic rates (Table 5 and Figure 19). In the presence of 10 molecules of DG, the doubling of TG resulted in a 14% decrease in PL hydrolysis but only

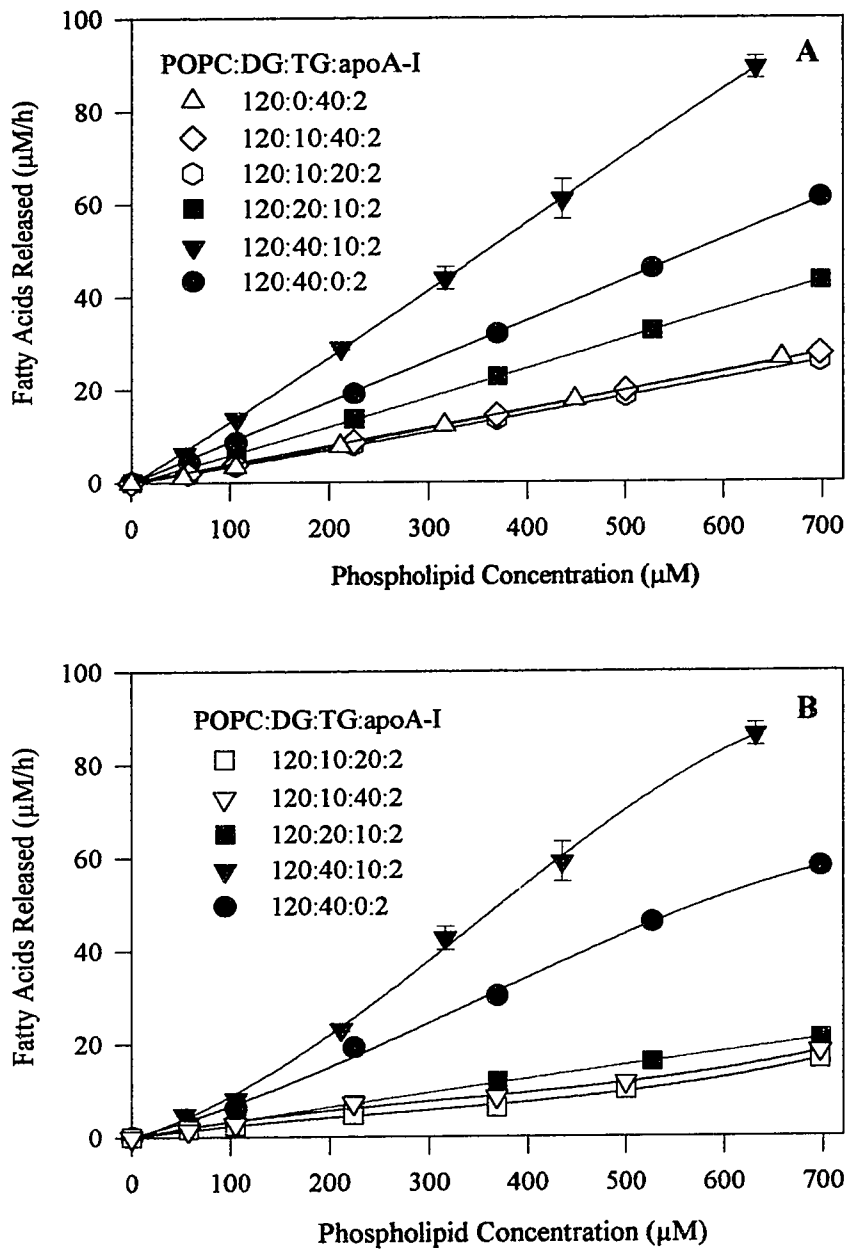


**Figure 19:** Effect of the diacylglycerol content of spherical Lp2A-I on HL activation. HL mediated hydrolysis of total lipids (Panel A) and diacylglycerol, DG, (Panel B) in Lp2A-I particles containing various amounts of DG and TG is shown. Lp2A-I stoichiometries after reisolation are shown in Table 5. Hydrolytic values are the mean  $\pm$ SD of triplicate determinations and are representative of at 3 different preparations of Lp2A-I.

an 8% increase in TG hydrolysis with the remaining 6% change due to an increase in DG. The absolute amount of DG hydrolysis did not change.

***Effect of Lp2A-I diacylglycerol content on hepatic lipase activity.*** Inclusion of a small amount (<10 molecules) of DG in Lp2A-I had no effect on overall rates of hydrolysis, relative to a particle with a similar amount of PC and TG (Figure 19A and Table 5). However, incorporation of this lipid significantly affected the substrate specificity of HL. Inclusion of 10 molecules of DG into a particle containing 40 molecules of TG significantly reduced the rate of hydrolysis for both PC and TG, in favour of a major increase in DG hydrolysis; 60% of the fatty acids liberated were from DG (Table 5 and Figure 19B). When the amount of TG was reduced from 40 to 20 molecules, but the DG maintained at 10 moles, the total hydrolytic activity remained unaffected but the relative hydrolytic rates for different lipids were modified. The percentage DG hydrolytic rates were slightly reduced, while the absolute amounts stayed the same, the TG hydrolysis was reduced by approximately 50% and PC hydrolysis was increased 1.6-fold (Table 5 and Figure 19).

When the DG content was increased and TG reduced to 120:20:10:2, POPC:DG:TG:apoA-I (mol:mol) the amount of total lipid hydrolysis was increased almost 2-fold. The absolute amount of DG hydrolyzed did not alter significantly from the particle containing 10 molecules of DG and 20 of TG, however there was a reduction in TG hydrolysis and an increase in PL hydrolysis (Figure 19A and B). The inclusion of DG in any of the Lp2A-I shifted the hydrolysis from the phospholipids and TG to a range between 50% to almost exclusively DG. The most dramatic results could be seen with the 120:40:10:2 POPC:DG:TG:apoA-I (mol:mol) particle, where most of the fatty acids liberated were from DG hydrolysis. Increasing the DG content to 40 molecules resulted in the highest total

hydrolytic rate of 143 nM FFA/h/ $\mu$ M POPC, 96% of which was due to DG hydrolysis. The same percent hydrolysis could be seen with the particle that had no TG. The particle with the highest DG content but devoid in TG, 120:40:2 POPC:DG:apoA-I mol:mol ratio, had a total hydrolytic rate of 89 nM fatty acids released/hr per  $\mu$ M POPC, that was almost entirely due to DG hydrolysis.

## DISCUSSION

### *Section I: HDL composition and structure*

The overall objective of this investigation was to determine how variations in the composition of HDL affect the catalytic activity of HL. To clearly resolve how HDL composition affects HL, it is important to understand how the composition of this lipoprotein affects its structural properties. Therefore, the objective of the first part of this project was to investigate the effect of DG and TG on the charge, conformation and stability of apoA-I in Lp2A-I.

In hyperTG subjects, the plasma TRL levels are elevated, the NAG content of HDL is increased, HDL<sub>2</sub> levels are decreased, HL activity is higher and atherosclerotic risk is increased (6-9). While it has been shown that HDL isolated from hyperTG patients and from individuals in postprandial states are better substrates for HL than those from normal fasting subjects (8, 9 & Figure 14) it is difficult to elucidate the exact factors that are involved in this catalytic activation within a native lipoprotein milieu. A series of experiments were designed, therefore, to test what effect DG and TG have on the conformation and stability of the primary apolipoprotein of HDL, apoA-I, and the overall surface potential within a homogeneous population of reconstituted lipoproteins. These well-defined substrates were then incubated with HL to elucidate structure/function relationships.

The study of HDL molecular structure and function has been hampered by the inherent heterogeneity of this lipoprotein class. It is difficult to elucidate the factor(s)

responsible for a specific effect if the population of particles under investigation is extremely diverse in size, charge and molecular composition. The use of well-defined, homogeneous preparations of reconstituted HDL particles, LpA-I or Lp2A-I, however, allows for one experimental variable to be altered at a time. This laboratory has successfully used both spherical and discoidal lipoprotein models to study the effect of various lipids on the charge,  $\alpha$ -helix content and stability of apoA-I (64, 65, 73, 75, 97).

Many studies have shown that changes in the lipid composition of HDL can affect both the conformation of apoA-I and its ability to promote cholesterol efflux, LCAT activation, interactions with CETP and CE-selective uptake (26-28, 71-73, 97, 98). Sparks *et al.* (65) have shown that an increase from a 1.2 to a 1.5 TG/CE molar ratio in spherical LpA-I decreases the  $\alpha$ -helix content and stability of apoA-I while increasing the surface potential from -8.0 mV to -7.5 mV. Altering the discoidal LpA-I charge with lipids such as PC and SPM has shown a negative correlation between LCAT activation and the surface potential values within a range of -7.5 to -8.5 mV (73). Braschi *et al.* (97) have found that the fractional catabolic rate (FCR) of HDL in rabbits is increased with particles that have a decreased negative charge. HDL particles containing DG and TG were the most negatively charged and exhibited the longest retention times (97).

Vieu *et al.* (33) suggest that DG may be an important constituent of HDL and may play an important role in the metabolism of these lipoproteins. These authors have shown that DG is the most abundant glyceride in HDL and that the molar ratios of DG/TG in HDL particles were from 2 to 7 for HDL<sub>2</sub> and HDL<sub>3</sub>, respectively. The data presented in this study on HDL-NAG confirms that DG is a major constituent of HDL,

however, much lower ratios of DG/TG were obtained than that reported by Vieu *et al.* (33). These differences may be due to inter-patient variation, as preliminary studies have shown considerable variation in this measurement among subjects (data not shown). This is supported by an earlier study with plasma from normolipidemics where DG was 1 to 10% that of the TG level (32).

In this study, incorporation of DG into Lp2A-I particles increased both the  $\alpha$ -helical content of apoA-I and the surface charge. Raising the DG from 0 to 40 molecules in a particle that contained 120:2 molar ratio of phospholipids to apoA-I increased the  $\alpha$ -helical content of the apoA-I from 62% to 69% while the surface charge changed from -9.1 to -11.0 mV. The more negative the surface potential, the greater the thermodynamic stability of apoA-I ( $R^2 = -0.88$ ). These differences in  $\alpha$ -helical content, stability and charge may arise from variations in the depth to which the  $\alpha$ -helices are embedded in the lipid surface of the particle. From sequence homology analyses of apoA-I, the  $\alpha$ -helices of this apoprotein are divided between Classes A and Y (58, 63). Class A  $\alpha$ -helices have clusters of positively charged amino acid residues at the polar-nonpolar interfaces and negatively charged residues at the polar faces (58, 63). It is believed that when the  $\alpha$ -helix is associated with phospholipids, the positive residues “snorkel” or extend in order to insert their charged residues into the aqueous environment (58, 63). This leaves the hydrophobic regions buried next to the acyl chains of the phospholipids while the negatively charged residues face the aqueous surface (58, 63). Class Y  $\alpha$ -helices have two negative and three positive residue clusters (58). In order for the surface charge of apoA-I to become more negative in the presence of DG, some of the positive residues at

the interface would have to become hidden and/or the negative charges would have to become more exposed. Burying the  $\alpha$ -helix further into the lipid surface layer could result in both a more negative charge and an increased  $\alpha$ -helix content as the positive residues would be less exposed and more of the protein would be associated with the hydrophobic environment of the acyl chains. These structural changes apparently give rise to a more stable structure, as evident from an increased  $\Delta G_D^\circ$  for apoA-I.

The conformation of apoA-I was evaluated in this study through the use of monoclonal antibodies. Numerous studies have used mAbs as a means of conformational analysis (reviewed in 60). mAbs have been described as sensitive probes in the study of apolipoprotein conformations as most mAbs raised against lipoproteins recognize epitopes formed from protein secondary or tertiary structures (60). Sparks *et al.* (73) have shown that surface lipids such as FC and PL have a global effect on charge,  $\alpha$ -helix content and stability of apoA-I, while Collet *et al.* (68) have shown which specific sequences seem most perturbed in native HDL. For example, with increased PL, the epitopes recognized by 2G11 are less exposed (68). With increased FC, the epitope recognized by 4H1 is more exposed but the one for 4A12 is less (68). With discoidal LpA-I, Bergeron *et al.* (69) found that increasing FC or decreasing PL increases the epitope immunoreactivity for 4H1 and A11. In this study, the area where DG reduced the epitope exposure the most was between amino acids 126 to 132 and 149 to 186. It is within these regions that the  $\alpha$ -helices may have become buried in the lipid layer, masking some of the positive residues and helping to decrease the LpA-I negative surface potential. In the region between 149-186, there are 10 positively and 7 negatively

charged residues (Figure 3) so a reduction in immunoreactivity here could decrease the surface potential. The presence of TG had an effect on the epitope exposure within the N-terminus of apoA-I. It was within the regions of the first 8 amino acids and between residues 25 through 82 that were hidden more than the control. This is also the area where the surface lipid, FC increased exposure in native HDL and discoidal LpA-I (68, 69), while PL decreased the immunoreactivity with the discs, indicating lipid compositional sensitivity for this epitope. DG content was also responsible for reduced antibody affinity within this region in the Lp2A-I model.

It is believed that DG partitions between the surface and the core of lipoproteins (100-102). Based on aggregation studies, Liu *et al.* (101) postulate that the presence of DG generates hydrophobic gaps within the surface monolayer of phospholipids. Amphipathic  $\alpha$ -helix-containing proteins, such as apoA-I are attracted to this environment and prevent aggregation in their model system. Further studies with  $^{13}\text{C}$ -NMR led to a model of DG intercalated between two phospholipid molecules (102). The authors suggest that apoproteins are more attracted to these hydrophobic gaps as there are less steric hindrances and charge interactions (100-102). In another report, Vieu *et al.* (33) proposed that most DG molecules are associated with the lipoprotein surface lipids, as 60% of the DG is accessible to cationic pancreatic lipase. The increased presence of DG at the surface of the lipoproteins can help explain why this lipid has a greater effect on apoA-I surface charge and  $\alpha$ -helix content than TG, which is predominantly found in the core. Indeed, the amount of DG in the Lp2A-I particles is directly related to the particle surface charge.

Apoprotein A-I is involved in cholesterol efflux (4, 16, 98), LCAT activation (4, 16, 98) and selective uptake of lipids through the actions of SR-B1/Cla-1 (26). The function of HDL in these various processes depends on the structure of apoA-I and its ability to assume different conformations (98). Within apoA-I, certain sequences are more important than others in promoting apoA-I mediated biological functions. In pre $\beta_1$ -HDL, there exists a unique conformation in the region of residues 137-144 that may be important for cholesterol efflux (16, 98). The neighbouring region of residues 143-165 is believed to interact with LCAT (16) with a potential regulatory site within residues 100-122 (73). This domain is also believed to be the putative cholesterol binding region (75), while phospholipid association is decreased if the central domain of apoA-I is deleted (70).

The differences in epitope exposure may help explain why DG has a major effect on the surface charge of the reconstituted particles. The regions affected by DG were more localized to the centre of the apoA-I molecule where more lipid binding and  $\alpha$ -helical structures are associated (68-70, 74). Fielding and Fielding (16) suggest that the LCAT association site for apoA-I is within residues 143-165. Since DG reduces the exposure of residues 126-132 and 149-186, HDL particles with increased DG may be poorer substrates for LCAT. This may effectively reduce the number of larger-sized HDL particles with CE-enriched cores. In addition, the presence of DG leads to increased HL activity, which may further reduce HDL<sub>2</sub> levels. If normolipidemics have molar ratios of DG/TG in HDL particles that range from 2 to 7 for HDL<sub>2</sub> and HDL<sub>3</sub>, respectively (33), then it is possible that hyperTG patients may have a higher content of DG in their HDL.

While a clinical study to investigate the ratio of DG to TG in hyperTG patients has not yet been performed, the data in this study suggests that elevated HDL-DG may promote the formation and the accumulation of small, dense HDL particles in these individuals.

## ***Section II: HDL and hepatic lipase***

Because HDL levels are inversely proportional to the risk of heart disease (reviewed in 4) and HL may affect HDL plasma levels (8, 9, 15), it is important to elucidate what factors may regulate the function of HL. While HL does not appear to require any cofactors, some investigators have shown an activation of this enzyme by apoA-II (96, 103, 104) and apoE (105). Other investigators, however, have found an inhibition of HL activity in the presence of apoA-II (106, 107). The physical environment, lipid and apolipoprotein content all appear to have an effect on the ability of HL to hydrolyze HDL. It appears that the results of substrate specificity studies with this enzyme differ depending on the model system used and the physical environment in which the substrate is presented. Laboda, Glick and Phillips (108) have shown that in lipid monolayers, triolein and dioleinphosphatidylethanolamine (PE) hydrolysis were similar and much greater than dioleinphosphatidylcholine (PC). They proposed that the polar group of the phospholipids might have had an effect on the rate of hydrolysis and possibly on the formation of the enzyme-substrate complex. Waite *et al.* (52) showed similar results. Azéma *et al.* (57) studied radiolabeled native HDL and showed that the rates of hydrolysis of [<sup>14</sup>C]dilinoleoylPE and [<sup>3</sup>H]triolein were approximately 30-50-fold higher than that of [<sup>14</sup>C]dioleoyl PC. They interpreted these results to mean that PE and TG were the preferred substrates for this enzyme in HDL, while PC was a less preferred substrate. This explanation appears correct only if the percentage of substrate hydrolyzed is examined rather than the absolute amount. When one considers the very small amounts of both TG and PE in an HDL particle, this hydrolysis appears to be minimal. More

recent data suggests that the amount of fatty acids liberated from HDL-PC is greater than that for PE and TG combined (54, 105). Data reported by Thuren *et al.* (54) suggests that PC is the preferred substrate of HL in HDL. In their study, the hydrolysis of phospholipids in HDL was 4 to 9-fold greater than that of TG.

In this investigation, a number of different substrates were used to elucidate the effect of different constituents on the catalytic regulation of human HL. A TG emulsion was utilized initially to follow the purification and to characterize the eluted fractions of HL from the heparin sepharose column (Figure 13A). Because this substrate bears little structural similarity to HDL, it was not the appropriate tool for the investigation of the substrate specificity of HL. Native lipoproteins, the *in vivo* substrates for HL, have been studied by various investigators (95, 96) and the data presented here for HDL is in accordance with previous reports. HDL<sub>2</sub>, the largest of the subspecies, is the best substrate for HL, followed by HDL<sub>3</sub> and then VHDL (Figure 14). One of the principal factors that accounts for differences seen between the hyperlipidemic HDL hydrolytic rates (0.75 to 6.2  $\mu\text{M}/\text{h}$ ) and those for a normolipidemic subject's HDL (0.4 to 3.7  $\mu\text{M}/\text{h}$ ) appears to be differences in the HDL NAG content. The hyperlipidemic subject had a 40% increase in NAG and a 20% increase in total cholesterol compared to the normolipidemic subject. This study shows that while cholesterol content has little effect on HL, HDL-NAG content may regulate the enzyme, although other factors cannot be ruled out.

Experiments with both native hyperTG and normolipidemic HDL show that HL is not primarily a TG-lipase (Figure 15). The hydrolysis of total fatty acids from the normolipidemic HDL occurred at a rate of 5.9  $\mu\text{M}/\text{h}$ , for the highest substrate

concentration, while those from TG were released 23 times more slowly. A similar trend was observed with the hyperTG HDL although the rates of fatty acid released from all lipids and TG were increased over those from the normolipidemic. The total hydrolysis was increased by 2 fold yet the TG hydrolysis was increased by more than 15 fold, in comparison to the normolipidemic HDL at a similar substrate concentration. The most obvious explanation for the difference in the absolute amounts of total FFA released between the hyperTG and normal HDL is that the increased FFA release is from TG. However, when taken together with the hydrolytic data from Figure 16 and Table 5, another explanation arises. Increasing the TG concentration in the presence of DG, does not appear to increase the total hydrolytic rates (Table 5), instead, the relative rates become redistributed so that PL hydrolysis contribution decreases while DG increases. Considering that in a normolipidemic HDL<sub>3</sub>, 49% of the FFA released are liberated from DG, it is possible that the increased hydrolytic rates in hyperTG HDL may not be only due to increased TG hydrolysis but increased DG hydrolysis as well, although other factors cannot be ruled out.

As with other interfacial enzymes, HL is sensitive to the composition and structure of its lipoprotein substrates. The surface lipids in HDL may generate an interfacial environment that can regulate the hydrolysis of PL or TG. Laboda, Glick and Phillips (108) showed that the interfacial surface pressure plays an important role in the accessibility of the enzyme to the substrate. The data presented here shows that the HL hydrolytic rate is proportional to the HDL surface charge ( $R^2 = 0.70$ ) and that the surface charge is related to the  $\alpha$ -helical content ( $R^2 = -0.88$ ). HL hydrolytic rates and  $\alpha$ -helical

content are more modestly related ( $R^2 = 0.46$ ). Other studies, however, have shown that HDL-core composition may also affect this enzyme as TG-enriched HDL<sub>2</sub> is the preferred substrate for HL (8, 9, 35). In this study, only SPM appeared to inhibit total hydrolysis compared to the control, in native HDL (Figure 17). The use of the reconstituted HDL for the study of TG hydrolysis did not show a significant change in TG hydrolytic rates with change in the concentration of surface lipids. TG hydrolysis may be somewhat constant due to similar partitioning of this core lipid to the surface of each reconstituted particle. PL hydrolysis may have changed but was not determined. Therefore, the increased hydrolysis observed with increased HDL-cholesterol content as reported by Azéma *et al.* (57), may reflect primarily PL hydrolysis.

Experiments with native normolipidemic HDL showed that HL primarily hydrolyzes DG and PL, while only 1-5% of the fatty acids liberated came from TG (Figure 16). This may explain why the introduction of human HL into an HL-deficient mouse had very little effect on plasma TG levels (109). The rates of TG hydrolysis for normotriglyceridemic Lp2A-I particles (that contained DG and < 20 mol TG/particle) were generally less than 10% of the total hydrolytic rates and less than 5% in the presence of substantial amounts of DG. HDL from normolipidemic patients exhibited similar total hydrolytic rates (10-36 nM/h/mM PL) to these Lp2A-I. Only when HDL was enriched in TG, in the absence of DG, did HL appear to act as a TG lipase. This appeared to be consistent with the increased TG hydrolysis seen with the hyperTG HDL tested earlier (Figure 15B). Increases in TG content, in the presence of DG, decreases PL hydrolysis but increases TG and DG hydrolysis, resulting in the same total hydrolysis. A 2-fold increase in total hydrolysis, therefore, is more likely due to an increase in DG as

increases in this lipid produce substantial increases total hydrolysis. Azéma *et al.* (57) also showed that enrichment of HDL with TG stimulated TG hydrolysis. Since HDL from both hyperTG and combined hyperlipidemic patients is enriched in NAG (4, 15, 39, 40), this compositional modification may partially account for the increased HL hydrolytic rates observed in incubations with HDL from these patients (8, 9, 35). However, while HDL-TG increases the rates of TG hydrolysis, TG has little effect on total lipid hydrolysis. The relative rates of TG and PL hydrolysis in HDL were much more significantly affected by the particle DG content (Figure 15). The ratios of DG to TG in hyperlipidemic subjects need to be measured to determine which constituent promotes the high HL hydrolytic rates in the plasma of these patients.

HDL-DG appears to be the preferred substrate for human HL *in vitro*. This study has shown that the hydrolytic activity of HL is increased with increased DG content of the Lp2A-I particles due to an increased hydrolysis of DG by HL. Since DG significantly affected the initial hydrolytic rates of HL, this suggested that the stimulation of HL by DG may be due to an increased affinity of this enzyme for this lipid. This was similar to the data reported by Waite *et al.* (110), which suggested that rat HL preferred substrates without polar head groups and may have a high affinity for DG. In the study presented here, DG hydrolytic rates represented about 30-49% of the total lipid hydrolysis in normolipidemic HDL. This was also close to what was observed for a normolipidemic reconstituted HDL particle containing 20 and 10 molecules of DG and TG, respectively. Furthermore, the surface charge of the Lp2A-I particles may influence the interaction between apoA-I and hepatic lipase. This study has shown that those particles with the most lipid-induced conformational changes in apoA-I, lower the surface potential and are

better substrates for HL.

Increases in the rates of DG hydrolysis by HL appeared to be inversely proportional to the hydrolysis of PL. When a small amount of TG was included in a particle containing DG and PL, there was a dramatic increase in the DG hydrolysis rate (Table 5). This increase in hydrolysis could be due to increased DG at the surface of the Lp2A-I particle. If TG displaced a portion of the 40 % of DG in the core of the lipoprotein, DG may move to the particle surface and become more accessible to HL. This effect was probably due more to an increase in substrate accessibility rather than an increase in the surface area. A corresponding increase in phospholipid, in the absence of DG, only resulted in a 5% increase of the hydrolytic rate (data not shown). If DG is predominantly located at the particle surface as previously proposed (33, 100), this would confirm the hypothesis that HL predominantly acts as a surface lipid lipase with normolipidemic HDL particles (54).

The origin of DG in plasma lipoprotein particles is unclear. Vieu *et al.* (33) showed evidence to suggest that it was unlikely that a plasma phospholipase C was responsible for DG synthesis in the plasma. Instead they suggested that DG accumulated in HDL due to reduced capability of HL to hydrolyze DG relative to TG. This hypothesis, however, was not supported by the studies of Waite and colleagues (52, 110) or by the observation in this study that human HL hydrolyzed DG much more rapidly than TG. Alternatively, HL may be involved in DG accumulation in HDL through its ability to promote the synthesis of DG. Early reports showed that HL also has a monoacylglycerol acyltransferase (MGAT) activity that can produce DG from 2 monoacylglycerol molecules or from one monoacylglycerol and a phospholipid (110).

Studies have shown that LPL liberated MGs accumulate *in vitro* (111), so it is possible that the HL MGAT activity may act cooperatively with lipoprotein lipase and convert its lipolytic degradative products in HDL into DG. In patients who are hyperTG and insulin resistant, the normal clearance of glucose and FFA from the plasma is reduced (36-41). The accumulation of NAG precursors could lead to increased synthesis of DG.

### *Section III: Physiological relevance*

Atherosclerosis is the major cause of mortality in industrialized nations (1, 2). There exists a strong inverse correlation, however, between coronary heart disease and HDL<sub>2</sub> plasma levels (1-5). Postheparin plasma HL activities and HDL particle size distribution have been shown to be associated, suggesting that HL plays a major role in the remodeling of HDL particles (8, 9, 15). In hyperTG patients, there is prolonged lipemia, low levels of HDL<sub>2</sub>, low activities of LPL and high activities of HL (35). The magnitude of the postprandial response is key to the TG-enrichment of HDL<sub>2</sub>, the preferred substrate for HL (34, 35). The response of adipose-tissue LPL is reduced in patients with insulin resistance (36) leading to prolonged postprandial lipemia and delayed clearance of glucose and FFA. These patients have increased levels of TG and because the levels of other NAG are masked by the methods of clinical lipid determinations, may have increased levels of DG. HL action on TG-enriched HDL<sub>2</sub> produces smaller, HDL<sub>3</sub>-sized particles and liberates lipid-poor apoA-I (29, 31). Through its propensity to promote the disassociation and clearance of apoA-I from HDL, HL may reduce plasma HDL levels and, thus, add to the risk of atherogenesis (29, 31, 112).

While this study suggests that elevated levels of HDL-DG may increase the risk of atherosclerosis, the factors responsible for regulating HDL-DG levels need to be characterized. DG accumulation in HDL could be due to an increased MGAT activity (110), utilization of excess FFA (36-41) or other mechanisms. Even though hyperTG patients have lower LPL activities than normal subjects, the absolute amount of hydrolysis could be higher in these individuals due to an increase in the substrate

availability for this enzyme. As MG is one of the products that accumulates following LPL hydrolysis, HL may utilize these lipids for the production of DG through its MGAT activity. In addition, hyperTG patients have excess FFA that could be used as substrates for DG synthesis. Transport of these FFA into the hepatocytes occurs readily, as does their incorporation into other lipids including PL, DG and TG preventing cellular internal damage. These additional lipids could then be repackaged into new lipoproteins adding to the increased synthesis of apoB-containing lipoproteins and elevated plasma levels of NAG observed in these patients.

The preferred substrate for HL is  $\alpha$ -migrating, TG-enriched HDL<sub>2</sub> (or NAG-enriched HDL<sub>2</sub>). The data presented here suggests that DG is better able than TG to induce the apoA-I conformational changes required for the more negative surface potential of  $\alpha$ -migrating HDL (-10.5 to -12.5 mV) and thus, DG may be more responsible than TG for the substrate selectivity and increased hydrolysis of HDL<sub>2</sub>. Increased HDL-DG content and its stimulation of HL, *in vivo*, could lead to an accumulation of small, dense HDL and lipid-poor apoA-I that could be cleared by the kidney. The promotion of low HDL<sub>2</sub> levels would be exacerbated if these negatively charged lipoproteins associated more with SR-B1/Cla-1, increased HDL-CE selective uptake and produced more lipid-poor apoA-I to be cleared from the plasma. The ability of LCAT to produce larger HDL<sub>2</sub> particles may also be impaired by specific conformational changes to apoA-I in the presence of DG. Increased amounts of DG, therefore, could lead to decreased amounts of HDL<sub>2</sub>, and as HDL<sub>2</sub> plasma levels are inversely proportional to atherosclerotic risk, potentially lead to an increase risk for the development of CAD.

#### ***Section IV: Future experiments***

One experiment that should be performed is a clinical measurement of hyperTG NAG levels in total plasma and within lipoprotein fractions. This study could help determine if high NAG levels are due to TG and/or DG and if DG is more proatherogenic than TG. The question still remains, “Is hypertriglyceridemia an *independent* risk factor for atherosclerosis?” so the investigation of specific NAG species may assist in this determination. If DG levels are increased more in hyperTG than in normals, it could be due to HL MGAT activity or a more complicated metabolic process that uses the increased FFA found in these patients. Other experiments could explore further the structure/function relationships of DG-containing particles. It would be interesting to test various LpA-I with SR-B1/Cla-1 expressing cells to see if the negatively charged DG-containing particles can increase selective uptake. The use of mAbs against apoA-I could map certain segments of the apoprotein for their interactions with SR-B1/Cla-1 and perhaps delineate further the domains that are responsible for the higher negative surface charge in the presence of DG.

## REFERENCES

1. Ross, R. 1993. The pathogenesis of atherosclerosis: a perspective for the 1990s. *Nature*. **362**: 801-809.
2. Breslow, J. L. 1996. Mouse models of atherosclerosis. *Science*. **272**: 685-688.
3. Sherwood, L. 1993. *Human physiology*, 2nd Ed., West Publishing Company, New York. pp. 291-295.
4. Tall, A. R. 1990. Plasma high density lipoproteins: metabolism and relationship to atherogenesis. *J. Clin. Invest.* **86**: 379-384.
5. Tall, A. R. 1992. Metabolic and genetic control of HDL cholesterol levels. *J. Inter. Med.* **231**: 661-668.
6. Ginsberg, H. N. 1997. Is hypertriglyceridemia a risk factor for atherosclerotic cardiovascular disease? A simple question with a complicated answer. *Ann. Intern. Med.* **126**: 912-914.
7. LaRosa, J. C. 1997. Triglycerides and coronary risk in women and the elderly. *Arch. Intern. Med.* **157**: 961-968.
8. Patsch, J. R., S. Prasad, A. M. Gotto, Jr., and W. Patsch. 1987. High density lipoprotein<sub>2</sub>: relationship of the plasma levels of this lipoprotein species to its composition, to the magnitude of postprandial lipemia, and to the activities of lipoprotein lipase and hepatic lipase. *J. Clin. Invest.* **80**: 341-347.
9. Patsch, J. R., G. Miesenböck, T. Hopperwieser, V. Hühlberger, E. Knapp, J. K. Dunn, A. M. Gotto, and W. Patsch. 1992. Relation of triglyceride metabolism and coronary artery disease: studies in the postprandial state. *Arterioscler. Thromb.* **12**: 1336-1345.
10. Davis, R. A. and J. E. Vance. 1996. Structure, assembly and secretion of lipoproteins. In D. E. Vance and J. E. Vance (eds.) *Biochemistry of Lipids, Lipoproteins and Membranes*. Elsevier Science B. V., New York. pp. 473-491.
11. Brown, M. S. and J. L. Goldstein. 1986. A receptor-mediated pathway for cholesterol homeostasis. *Science*. **232**: 34-47.
12. Assman, G., A. von Eckardstein. and H. Funke. 1992. Mutations in apolipoprotein genes and HDL metabolism. In M. Rosseneu (ed.) *Structure and function of apolipoproteins*. CRC Press, Inc., Boca Raton. pp. 85-121.
13. Cohen, J. C., Z. Wang, S. M. Grundy, M. R. Stoesz, and R. Guerra. 1994. Variation

at the hepatic lipase and apolipoprotein AI/CII/AIV Loci is a major cause of genetically determined variation in plasma HDL cholesterol levels. *J. Clin. Invest.* **94**: 2377-2384.

14. Breslow, J. L. 1995. Familial disorders of high-density lipoprotein metabolism. In C. R. Scriver, A. L. Beaudet, W. S. Sly and D. Valle (eds.) *The metabolic and molecular basis of inherited disease*, 7th Ed., McGraw-Hill, Inc., New York. pp. 2031-2052.

15. Applebaum-Bowden, D., S. M. Haffner, P. W. Wahl, J. Hoover, G. R. Warnick, J. J. Albers, and W. R. Hazzard. 1985. Postheparin plasma triglyceride lipases. Relationships with very low density lipoprotein triglyceride and high density lipoprotein<sub>2</sub> cholesterol. *Arteriosclerosis* **5**: 273-282.

16. Fielding, C. J. and P. E. Fielding. 1995. Molecular physiology of reverse cholesterol transport. *J. Lipid Res.* **36**: 211-228.

17. Sparks, D.L. and M. C. Phillips. 1992. Quantitative measurement of lipoprotein surface charge by agarose gel electrophoresis. *J. Lipid Res.* **33**: 123-130.

18. Davidson, W. S., D. L. Sparks, S. Lund-Katz and M. C. Phillips. 1994. The molecular basis for the difference in charge between pre- $\beta$ - and  $\alpha$ -migrating high density lipoproteins. *J. Biol. Chem.* **269**: 8959-8965.

19. Bensadoun, A. and D. E. Berryman. 1996. Genetics and molecular biology of hepatic lipase. *Current Opinion Lipidology.* **7**: 77-81.

20. Scanu, A. M. 1972. Structural studies on serum lipoproteins. *Biochim. Biophys. Acta.* **265**: 471-508.

21. Skinner, E. R. 1992. The separation and analysis of high-density lipoprotein (HDL) and low-density lipoprotein (LDL) subfractions. In C. A. Converse and E. R. Skinner (eds). *Lipoprotein Analysis: A practical approach*. IRL Press at Oxford University Press. New York.

22. Nichols, A. V., R. M. Krauss, and T. A. Musliner. 1986. Nondenaturing polyacrylamide gradient gel electrophoresis. *Meth. Enzymol.* **128**: 417-431.

23. Verdery, R. B., D. F. Benham, H. L. Baldwin, A. P. Goldberg, and A. V. Nichols. 1989. Measurement of normative HDL subfraction cholesterol levels by Gaussian summation analysis of gradient gels. *J. Lipid Res.* **30**: 1085-1095.

24. Scheider, W. J. 1996. Removal of lipoproteins from the plasma. In D. E. Vance and J. E. Vance (eds.) *Biochemistry of Lipids, Lipoproteins and Membranes*. Elsevier Science B. V., New York. pp. 517-541.

25. Glass, C., R. C. Pittman, D. B. Weinstein, and D. Steinberg. 1983. Dissociation of tissue uptake of cholesterol ester from that of apoprotein A-I of rat plasma high density lipoprotein: selective delivery of cholesterol ester to liver, adrenal, and gonad. *Proc. Natl. Acad. Sci. USA*. **80**: 5435-5439.
26. Rigotti, A., B. Trigatti, J. Babitt, M. Penman, S. Xu, and M. Krieger. 1997. Scavenger receptor B1 - a cell surface receptor for high density lipoproteins. *Current Opinion Lipidology*. **8**: 181-188.
27. Kadowaki, H., G. M. Patton, and S. J. Robins. 1992. Metabolism of high density lipoprotein lipids by the rat liver: evidence for participation of hepatic lipase in the uptake of cholesteryl ester. *J. Lipid Res*. **33**: 1689-1698.
28. Marques-Vidal, P., C. Azéma, X. Collet, H. Chap, and B. P. Perret. 1991. Hepatic lipase-mediated hydrolysis versus liver uptake of HDL phospholipids and triacylglycerols by the perfused rat liver. *Biochim. Biophys. Acta*. **1082**: 185-194.
29. Barrans, A. X. Collet, R. Barbaras, B. Jaspard, J. Manent, C. Vieu, H. Chap, and B. Perret. 1994. Hepatic lipase induces the formation of pre- $\beta_1$  high density lipoprotein (HDL) from triacylglycerol-rich HDL<sub>2</sub>. *J. Biol. Chem*. **269**: 11572-11577.
30. Horowitz, B. S., I. J. Goldberg, J. Merab, T. M. Vanni, R. Ramakrishnan, and H. N. Ginsberg. 1993. Increased plasma and renal clearance of an exchangeable pool of apolipoprotein A-I in subjects with low levels of high density lipoprotein cholesterol. *J. Clin. Invest*. **91**: 1743-1752.
31. Clay, M. A., H. H. Newman, and P. J. Barter. 1991. Hepatic lipase promotes a loss of apolipoprotein A-I from triglyceride-enriched human high density lipoproteins during incubation in vitro. *Arterioscler. Thromb*. **11**: 415-422.
32. Fielding, B. A., S. M. Humphreys, and K. N. Frayn. 1993. Mono- and diacylglycerol concentrations in human plasma in relation to lipoprotein lipase. *Biochem. Soc. Trans.* (Pt. 3.) **3**: 235S.
33. Vieu, C., B. Jaspard, R. Barbaras, J. Manent, H. Chap, B. Perret, and X. Collet. 1996. Identification and quantification of diacylglycerols in HDL and accessibility to lipase. *J. Lipid Res*. **37**: 1153-1161.
34. Hamsten, A. 1990. Hypertriglyceridemia, triglyceride-rich lipoproteins and coronary heart disease. *Baillière's Clin. Endocrinol. Metabol*. **4**: 895-922.
35. Kirchmair, R., C. F. Ebenbichler, and J. R. Patsch. 1995. Post-prandial lipaemia. *Baillière's Clin. Endocrinol. Metabol*. **9**: 705-719.

36. Reaven, G. M. 1995. Pathophysiology of insulin resistance in human disease. *Physiol. Rev.* **75**: 473-486.
37. Bernlohr, D. A. and M. A. Simpson. 1996. Adipose tissue and lipid metabolism. In D. E. Vance and J. E. Vance (eds.) *Biochemistry of Lipids, Lipoproteins and Membranes*. Elsevier Science B. V., New York. pp. 257-281.
38. Lewis, G. F. and G. Steiner. 1996. Hypertriglyceridemia and its metabolic consequences as a risk factor atherosclerotic cardiovascular disease in non-insulin-dependent diabetes mellitus. *Diabetes Metab. Rev.* **12**: 37-56.
39. Cominacini, L., U. Garbin, A. Davoli, M. Campagnola, A. DeSantis, C. Pasini, A. M. Pastorino and O. Bosello. 1993. High-density lipoprotein cholesterol concentrations and postheparin hepatic and lipoprotein lipases in obesity: relationships with plasma insulin levels. *Ann. Nutr. Metab.* **37**: 175-184.
40. Jeppesen, J. Hollenbeck, C. B., M.-Y. Zhou, A. M. Coulston, C. Jones, Y.-D. I. Chen, and G. M. Reaven. 1995. Relation between insulin resistance, hyperinsulinemia, postheparin plasma lipoprotein lipase activity, and postprandial lipemia. *Arterioscler. Thromb. Vasc. Biol.* **15**: 320-324.
41. Eckel, R. H. and T. J. Yost. 1987. Weight reduction increases adipose tissue lipoprotein lipase responsiveness in obese women. *J. Clin. Invest.* **80**: 245-246.
42. Jackson, R. L. 1983. Lipoprotein lipase and hepatic lipase. In P. D. Boyer (ed.) *The Enzymes*. 3rd ed. Academic Press, New York. **16**: 141-181.
43. Cooper, A. D. 1997. Hepatic uptake of chylomicron remnants. *J. Lipid Res.* **38**: 2173-2192.
44. Verhoeven, A. J. M. and Jansen, H. 1994. Hepatic lipase mRNA is expressed in rat and human steroidogenic organs. *Biochim. Biophys. Acta.* **1211**: 121-124.
45. Datta, S., C.-C. Luo, W.-H. Li, P. VanTuinen, D. H. Ledbetter, M. A. Brown, S.-H. Chen, S. Liu, and L. Chan. 1988. Human hepatic lipase: cloned cDNA, sequence, restriction fragment length polymorphisms, chromosomal location, and evolutionary relationships with lipoprotein lipase and pancreatic lipase. *J. Biol. Chem.* **263**: 1107-1110.
46. Martin, G. A., S. J. Busch, G. D. Meredith, A. D. Cardin, D. T. Blankenship, S. J. T. Mao, A. E. Rechten, C. W. Woods, M. M. Racke, M. P. Schafer, M. C. Fitzgerald, D. M. Burke, M. A. Flanagan, and R. L. Jackson. 1988. Isolation and cDNA sequence of human postheparin plasma hepatic triglyceride lipase. *J. Biol. Chem.* **263**: 10907-10914.
47. Hill, J. S., R. C. Davis, D. Yang, J. Wen, J. S. Philo, P. H. Poon, M. L. Phillips, E. S.

- Kempner, and H. Wong. 1996. Human hepatic lipase subunit structure determination. *J. Biol. Chem.* **271**: 22931-22936.
48. Tikkanen, M. J. and E. A. Nikkila. 1987. Regulation of hepatic lipase and serum lipoproteins by sex steroids [Review]. *Am. Heart J.* **113**: 562-567.
49. Hegele, R. A., J. A. Little, C. Vezina, G. F. Maguire, L. Tu, T. S. Wolever, D. J. A. Jenkins, and P. W. Connelly. 1993. Hepatic lipase deficiency: clinical, biochemical, and molecular genetic characteristics. *Arterioscler. Thromb.* **13**: 720-728.
50. Homanics, G. E., H. V. de Silva, J. Osada, S. H. Zhang, H. Wong, J. Borensztajn, and N. Maeda. 1995. Mild dyslipidemia in mice following targeted inactivation of the hepatic lipase gene. *J. Biol. Chem.* **270**: 2974-2980.
51. Busch, S. J., R. L. Barnhart, G. A. Martin, M. C. Fitzgerald, M. T. Yates, S. J. T. Mao, C. E. Thomas, and R. L. Jackson. 1994. Human hepatic triacylglycerol lipase expression reduces high density lipoprotein and aortic cholesterol in cholesterol-fed transgenic mice. *J. Biol. Chem.* **269**: 16376-16382.
52. Waite M., T. Y. Thuren, R. W. Wilcox, P. J. Sisson, and G. L. Kucera. 1991. Purification and substrate specificity of rat hepatic lipase. *Meth. Enzymol.* **197**: 331-339.
53. Mahendra, K. J., M. H. Gelb, J. Rogers, and O. G. Berg. 1995. Kinetic basis for interfacial catalysis by phospholipase A<sub>2</sub>. *Meth. Enzymol.* **249**: 567-614.
54. Thuren, T., R. W. Wilcox, P. Sisson, and M. Waite. 1991. Hepatic lipase hydrolysis of lipid monolayers: regulation by apolipoproteins. *J. Biol. Chem.* **266**: 4853-4861.
55. Santamarina-Fojo, S. and K. A. Dugi. 1994. Structure, function and role of lipoprotein lipase in lipoprotein metabolism. *Current Opinion Lipidology.* **5**: 117-125.
56. Simard, G., B. Perret, S. Durand, X. Collet, H. Chap, and L. Douste-Blatzy. 1989. Phosphatidylcholine and triacylglycerol hydrolysis in HDL as induced by hepatic lipase: modulation of the phospholipase activity by changes in the particle surface or in the lipid core. *Biochim. Biophys. Acta* **1001**: 225-233.
57. Azéma, C., P. Marques-Vidal, A. Lespine, G. Simard, H. Chap, and B. Perret. 1990. Kinetic evidence for phosphatidylethanolamine and triacylglycerol as preferential substrates for hepatic lipase in HDL subfractions: modulation by changes in the particle surface, or in the lipid core. *Biochim. Biophys. Acta* **1046**: 73-80.
58. Segrest, J. P., M. K. Jones, H. De Loof, C. G. Brouillette, Y. V. Venkatachalapathi, and G. M. Anantharamaiah. 1992. The amphipathic helix in the exchangeable apolipoproteins: a review of secondary structure and function. *J. Lipid Res.* **33**: 141-166.

59. Bairoch A. and R. Apweiler. 1997. The SWISS-PROT protein sequence data bank and its supplement TrEMBL. *Nucleic Acids Res.* **25**: 31-36.
60. Marcel, Y. L., E. Rassart, L. Brissette, and R. W. Milne. 1992. Immunochemical studies of apolipoprotein structure and function. In M. Rosseneu (ed.) *Structure and function of apolipoproteins*. CRC Press, Inc., Boca Raton. pp. 363-399.
61. Marcel, Y. L., P. B. Provost, H. Koa, E. Raiffaï, N. Vu Dac, J.-C. Fruchart, and E. Rassart. 1991. The epitopes of apolipoprotein A-I define distinct structural domains including a mobile middle region. *J. Biol. Chem.* **266**: 3644-3653.
62. Sparks, D. L., M. C. Phillips, and S. Lund-Katz. 1992. The conformation of apolipoprotein A-I in discoidal and spherical recombinant high density lipoprotein particles. <sup>13</sup>C NMR studies of lysine ionization behavior. *J. Biol. Chem.* **267**: 25830-25838.
63. Borhani, D. W., D. P. Rogers, J. A. Engler, and C. G. Brouillette. 1997. Crystal structure of truncated human apolipoprotein A-I suggests a lipid-bound conformation. *Proc. Natl. Acad. Sci.* **94**: 12291-12296.
64. Sparks, D. L., S. Lund-Katz, and M. C. Phillips. 1992. The charge and structural stability of apolipoprotein A-I in discoidal and spherical recombinant high density lipoprotein particles. *J. Biol. Chem.* **267**: 25839-25847.
65. Sparks, D. L., W. S. Davidson, S. Lund-Katz and M. C. Phillips. 1995. Effects of the neutral lipid content of high density lipoprotein on apolipoprotein A-I structure and particle stability. *J. Biol. Chem.* **270**: 26910-26917.
66. Ishida, B. Y., J. Frolich, C. J. Fielding. 1987. Prebeta-migrating high density lipoprotein: quantitation in normal and hyperlipidemic plasma by solid phase radioimmunoassay following electrophoretic transfer. *J. Lipid Res.* **28**: 778-786.
67. Zhao, Y., D. L. Sparks and Y. L. Marcel. 1996. Specific phospholipid association with apolipoprotein A-I stimulates cholesterol efflux from human fibroblasts: studies with reconstituted sonicated lipoproteins. *J. Biol. Chem.* **271**: 25145-25151.
68. Collet, X., B. Perret, G. Simard, E. Raiffaï, and Y. Marcel. 1991. Differential effects of lecithin and cholesterol on the immunoreactivity and conformation of apolipoprotein A-I in high density lipoproteins. *J. Biol. Chem.* **266**: 9145-9152.
69. Bergeron, J., P. G. Frank, D. Scales, Q.-H. Meng, G. Castro, and Y. L. Marcel. 1995. Apolipoprotein A-I conformation in reconstituted discoidal lipoproteins varying in phospholipid and cholesterol content. *J. Biol. Chem.* **270**: 27429-27438.
70. Frank, P. G., J. Bergeron, F. Emmanuel, J.-P. Lavigne, D. L. Sparks, P. Deneffe, E.

- Rassart, and Y. L. Marcel. 1997. Deletion of central  $\alpha$ -helices in human apolipoprotein A-I: effect on phospholipid association. *Biochemistry*. **36**: 1798-1806.
71. Banka, C. L., D. J. Bonnet, A. S. Black, R. S. Smith, and L. K. Curtiss. 1991. Localization of an apolipoprotein A-I epitope critical for activation of lecithin-cholesterol acyltransferase. *J. Biol. Chem.* **266**: 23886-23892.
72. Meng, Q.-H., L. Calabresi, J.-C. Fruchart, and Y. L. Marcel. 1993. Apolipoprotein A-I domains involved in the activation of lecithin:cholesterol acyltransferase. Importance of the central domain. *J. Biol. Chem.* **268**: 16966-16973.
73. Sparks, D. L. P. Frank, and T. A.-M. Neville. 1998. Effect of the surface lipid content of reconstituted LpA-I on apolipoprotein A-I structure and lecithin:cholesterol acyltransferase activity. *Biochim. Biophys. Acta.* **1390**: 160-172.
74. Fielding, P. E., M. Kawano, A. L. Catapano, A. Zoppo, S. Marcovina, and C. J. Fielding. 1994. Unique epitope of apolipoprotein A-I expressed in pre- $\beta$ -1 high density lipoprotein and its role in the catalyzed efflux of cellular cholesterol. *Biochem.* **33**: 6981-6985.
75. Sparks, D. L., W. S. Davidson, S. Lund-Katz, and M. C. Phillips. 1993. Effect of Cholesterol on the charge and structure of apolipoprotein A-I in recombinant high density lipoprotein particles. *J. Biol. Chem.* **268**: 23250-23257.
76. Jonas, A. 1986. Reconstitution of high-density lipoproteins. *Meth. Enzymol.* **128**: 553-567.
77. Atkinson, D. and D. M. Small. 1986. Recombinant lipoproteins: implications for structure and assembly of native lipoproteins. *Ann. Rev. Biophys. Chem.* **15**: 403-456.
78. Pownall, H. J., J. B. Massey, J. T. Sparrow, and A. M. Jr. Gotto. 1987. In Plasma Lipoproteins. Elsevier, Amsterdam. pp. 95-127.
79. Sloop, C. H., L. Dory, and P. S. Roheim. 1987. Interstitial fluid lipoproteins. *J. Lipid Res.* **28**: 225-237.
80. Jonas, A. 1991. Lecithin-cholesterol acyltransferase in the metabolism of high-density lipoproteins. *Biochim. Biophys. Acta* **1084**: 205-220.
81. Ritter, M. C. and A. M. Scanu. 1977. Structural changes in human serum high density lipoprotein-3 attending incubation with blood leukocytes. *J. Biol. Chem.* **252**: 1208-1216.
82. Sparks, D. L. and P. H. Pritchard. 1989. The neutral lipid composition and size of recombinant high density lipoproteins regulates lecithin:cholesterol acyltransferase

activity. *Biochem. Cell. Biol.* **67**: 358-364.

83. Sparks, D. L. and P. H. Pritchard. 1989. Transfer of cholesteryl ester into high density lipoprotein by cholesteryl ester transfer protein: effect of HDL lipid and apoprotein content. *J. Lipid Res.* **30**: 1491-1498.

84. Jones, S. M. A. and M. P. Rogers. 1985. Reconstituted high density lipoprotein behaviour is modified by the nature of the lipid vesicle. *FEBS Lett.* **180**: 66-68.

85. Pittman, R. C., C. K. Glass, D. Atkinson, and D. Small. 1987. Synthetic high density lipoprotein particles. Application to studies of the apoprotein specificity for selective uptake of cholesterol esters. *J. Biol. Chem.* **262**: 2435-2442.

86. Sparks, D. L., J. Frohlich, A. G. Lacko, and P. H. Pritchard. 1989. Relationship between cholesteryl ester transfer activity and high density lipoprotein composition in hyperlipidemic patients. *Atherosclerosis.* **77**: 183-191.

87. Guérin, M., Bruckert, É., Dolphin, P. J., Turpin, G., Chapman, M. J. 1996. Fenofibrate reduces plasma cholesteryl ester transfer from HDL to VLDL and normalizes the atherogenic, dense LDL profile in combined hyperlipidemia. *Arterioscler. Thromb. Vasc. Biol.* **16**: 763-772.

88. Sparks, D. L., G. M. Anantharamaiah, J. P. Segrest and M. C. Phillips. 1995. Effect of the cholesterol content of reconstituted LpA-I on lecithin:cholesterol acyltransferase activity. *J. Biol. Chem.* **270**: 5151-5157.

89. Brewer, H. B., Jr., R. Ronan, M. Meng, and C. Bishop. 1986. Isolation and characterization of apolipoproteins A-I, A-II, and A-IV. *Meth. Enzymol.* **128**: 223-235.

90. Markwell, M. K., S. M. Haas, L. L. Bieber, and N.E. Tolbert. 1978. A modification of the Lowry procedure to simplify protein determination in membrane and lipoprotein samples. *Anal. Biochem.* **87**: 206-210.

91. Sokoloff, L. and G. H. Rothblatt. 1974. Sterol to phospholipid molar ratios of L cells with qualitative and quantitative variations of cellular sterol. *Proc. Soc. Nat. Exp. Biol. Med.* **146**: 1166-1172.

92. Ehnholm, C. and T. Kuusi. 1986. Preparation, characterization, and measurement of hepatic lipase. *Methods Enzymol.* **129**: 716-738.

93. Belfrage, P. and M. Vaughan. 1969. Simple liquid-liquid partition system for isolation of labeled oleic acid from mixtures with glycerides. *J. Lipid Res.* **10**: 341-348.

94. Cheng, C. F., A. Bensadoun, T. Bersot, J. S. T. Hsu, and K. H. Melford. 1985. Purification and characterization of human lipoprotein lipase and hepatic triglyceride

lipase. Reactivity with monoclonal antibodies to hepatic triglyceride lipase. *J. Biol. Chem.* **260**: 10720-10727.

95. Shirai, K., R. L. Barnhart, and R. L. Jackson. 1981. Hydrolysis of human plasma high density lipoprotein<sub>2</sub>- phospholipids and triglycerides by hepatic lipase. *Biochem. Biophys. Res. Commun.* **100**: 591-599.

96. Mowri, H. O., J. R. Patsch, J.R., A. M. Gotto, Jr., and P. W Patsch. 1996. Apolipoprotein A-II influences the substrate properties of human HDL<sub>2</sub> and HDL<sub>3</sub> for hepatic lipase. *Arterioscler. Thromb. Vascular Biol.* **16**: 755-762.

97. Braschi, S., T. A.-M. Neville, M.-C. Vohl, and D. L. Sparks. 1998. Apolipoprotein A-I charge and conformation regulate high density lipoprotein clearance in rabbits. Submitted to *J. Lipid Res.*

98. Fielding, P. E. and C. J. Fielding. 1995. Dynamics of lipoprotein transport in the human circulatory system. In D. E. Vance and J. E. Vance (eds.) *Biochemistry of Lipids, Lipoproteins and Membranes*. Elsevier Science B. V., New York. pp. 495-516.

99. Xu, S., M. Laccotripe, X, Huang, A. Rigotti, V. I. Zannis, and M. Krieger. 1997. Apolipoproteins of HDL can directly mediate binding to the scavenger receptor SR-B1, an HDL receptor that mediates selective lipid uptake. *J. Lipid Res.* **38**: 1289-1298.

100. Ryan, R. O. 1996. Structural studies of lipoproteins and their apolipoprotein components. *Biochem. Cell Biol.* **74**, 155-164.

101. Liu H., D. G. Scraba, R. O. Ryan. 1993. Prevention of phospholipase-C induced aggregation of low density lipoprotein by amphipathic apolipoproteins. *FEBS Letters.* **316**: 27-33.

102. Wang, J., H. Liu, B. D. Sykes, R. O. Ryan. 1995. Identification and localization of two distinct microenvironments for the diacylglycerol component of lipophorin particles by <sup>13</sup>C NMR. *Biochemistry* **34**: 6755-6761.

103. Jahn, C. E., J. C. Osborne, Jr., E. J. Schaefer, and H. B. Brewer, Jr. 1983. Activation of the enzyme activity of hepatic lipase by apolipoprotein A-II: characterization of a major component of high density lipoprotein as the activating plasma component *in vitro*. *Eur. J. Biochem.* **131**: 25-29.

104. Mowri, H. -O., W. Patsch, L. C. Smith, A. M. Gotto, Jr., and J. R. Patsch. 1992. Different reactivities of high density lipoprotein<sub>2</sub> subfractions with hepatic lipase. *J. Lipid Res.* **33**: 1269-1279.

105. Thuren, T., K. H. Weisgraber, P. Sisson, and M. Waite. 1992. Role of apolipoprotein E in hepatic lipase catalyzed hydrolysis of phospholipid in high-density lipoproteins.

*Biochemistry* **31**: 2332-2338.

106. Zhong, S., I. Goldberg, C. Bruce, E. Rubin, J. L. Breslow, and A. J. Tall. 1994. Human apoA-II inhibits the hydrolysis of HDL and the decrease of HDL size induced by hypertriglyceridemia and cholesteryl ester transfer protein in transgenic mice. *J. Clin. Invest.* **94**: 2457-2467.

107. Weng, W. and J. L. Breslow. 1996. Dramatically decreased HDL, increased remnant clearance, and insulin hypersensitivity in apoA-II knockout mice suggest a complex role for apoA-II. *Proc. Natl. Acad. Sci.* **93**: 14788-14794.

108. Laboda, H. M., J. M. Glick, and M. C. Phillips. 1986. Hydrolysis of lipid monolayers and the substrate specificity of hepatic lipase. *Biochim. Biophys. Acta* **876**: 233-242.

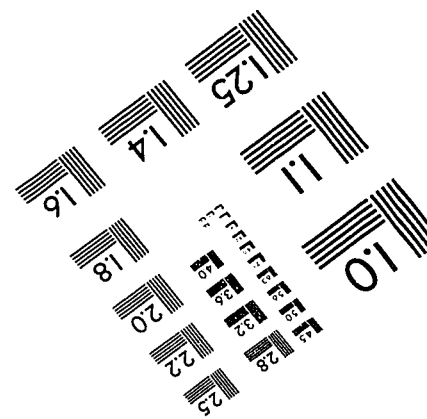
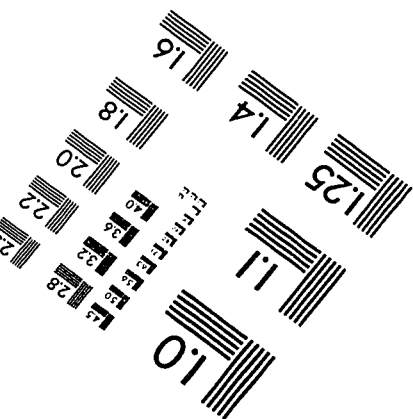
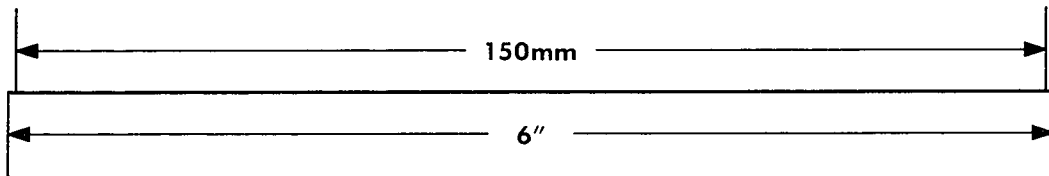
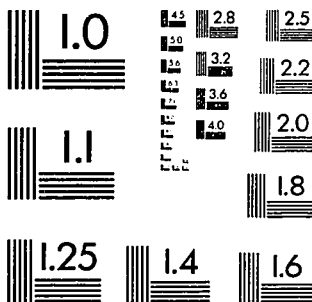
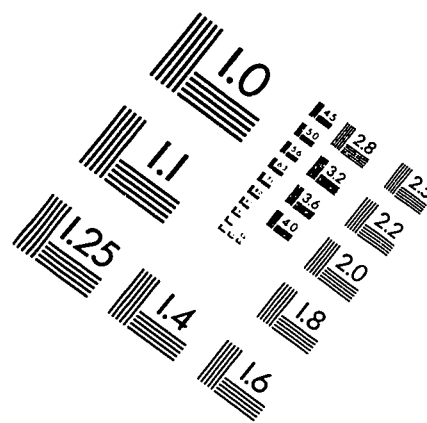
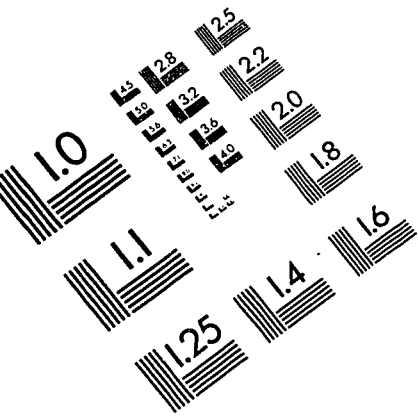
109. Kobayashi, J., D. Applebaum-Bowden, K. A. Dugi, D. R. Brown, V. S. Kashyap, C. Parrott, C. Duarte, N. Maeda, and S. Santamarina-Fojo. 1996. Analysis of protein structure-function in vivo: adenovirus-mediated transfer of lipase lid mutants in hepatic lipase-deficient mice. *J. Biol. Chem.* **271**: 26296-26301.

110. Waite, M. and P. Sisson. 1973. Utilization of neutral glycerides and phosphatidyl-ethanolamine by the phospholipase A-1 of the plasma membranes of rat liver. *J. Biol. Chem.* **248**: 7985-7992.

111. Ikeda, Y., A. Takagi, and A. Yamamoto. 1989. Purification and characterization of lipoprotein lipase and hepatic triglyceride lipase from postheparin plasma: production of monospecific antibody to the individual lipase. *Biochim. Biophys. Acta.* **1003**: 254-269.

112. Brinton, E. A., S. Eisenberg, and J. L. Breslow. 1994. Human HDL cholesterol levels are determined by apoA-I fractional catabolic rate, which correlates inversely with estimates of HDL particle size. Effects of gender, hepatic and lipoprotein lipases, triglyceride and insulin levels, and body fat distribution. *Arterioscler. Thromb.* **14**: 707-720.

# IMAGE EVALUATION TEST TARGET (QA-3)



APPLIED IMAGE, Inc  
1653 East Main Street  
Rochester, NY 14609 USA  
Phone: 716/482-0300  
Fax: 716/288-5989

© 1993, Applied Image, Inc., All Rights Reserved